THE REPUBLIC OF TURKEY

MUĞLA SITKI KOÇMAN UNIVERSITY

GRADUATE SCHOOL OF NATURAL AND

APPLIED SCIENCES

DEPARTMENT OF GEOLOGICAL ENGINEERING

A MATRIX APPROACH FOR VISUALISATION OF
SELECTED PHYSICO-CHEMICAL PROPERTIES OF
AKYAKA (GÖKOVA) KARST SPRINGS, MUĞLA

MASTER THESIS

ERAY AVCI

JANUARY 2016

MUĞLA

# MUGLA SITKI KOÇMAN ÜNİVERSİTESİ
## Fen Bilimleri Enstitüsü

## TEZ ONAYI

**ERAY AVCI** tarafından hazırlanan **A MATRIX APPROACH FOR VISUALISATION OF SELECTED PHYSICO-CHEMICAL PROPERTIES OF AKYAKA (GÖKOVA) KARST SPRINGS, MUĞLA** başlıklı tezinin, 21/01/2016 tarihinde aşağıdaki jüri tarafından Jeoloji Mühendisliği Anabilim Dalı'nda yüksek lisans derecesi için gerekli şartları sağladığı oybirliği/oyçokluğu ile kabul edilmiştir.

## TEZ SINAV JÜRİSİ

Yrd. Doç. Dr. Hüseyin KARAKUŞ **(Jüri Başkanı)**          İmza:

Uygulamalı Jeoloji Anabilim Dalı,
Dumlupınar Üniversitesi, Kütahya

Yrd. Doç. Dr. Bedri KURTULUŞ **(Danışman)**          İmza:

Jeoloji Mühendisliği Anabilim Dalı,
Muğla Sıtkı Koçman Üniversitesi, Muğla

Doç. Dr. Evren TUNCA **(Üye)**          İmza:

Deniz Bilimleri ve Teknolojisi Mühendisliği Anabilim Dalı

Ordu Üniversitesi, Ordu

## ANA BİLİM DALI BAŞKANLIĞI ONAYI

Yrd. Doç. Dr. Bedri KURTULUŞ          İmza:

Jeoloji Mühendisliği Ana Bilim Dalı Başkanı,
Muğla Sıtkı Koçman Üniversitesi, Muğla

Yrd. Doç. Dr. Bedri KURTULUŞ          İmza:

Jeoloji Mühendisliği Anabilim Dalı,
Muğla Sıtkı Koçman Üniversitesi, Muğla

Savunma Tarihi: 21/01/2016

I declare all results and information in this document have been obtained and presented in accordance with scientific and academic ethic rules. I also declare that all original information and results belong to someone else that were not achieved within the study of this thesis were referenced by ethic rules of academy and science.

<div align="right">

Eray AVCI

21/01/2016

</div>

# ÖZET

## MUĞLA, AKYAKA (GÖKOVA) KARST KAYNAKLARININ
## SEÇİLEN FİZİKO-KİMYASAL PARAMETRELERİNİN
## MATRİS YÖNTEMİ YAKLAŞIMI İLE GÖSTERİLMESİ

Eray AVCI

Bu tez çalışması, Muğla ili Akyaka mahallesi sınırları içerisinde bulunan Akyaka karst kaynaklarının, 2015 Nisan ve Eylül ayları arası, su sıcaklığı, özgül elektriksel iletkenlik ve pH değerlerinin ölçülmesi ile bölgede mevcut olan deniz suyu karışım mekanizmasının anlaşılmasına katkı sağlamak amacı ile yapılmıştır.

Ölçümlere başlangıç tarihi olarak kaynakların boşalıma geçtiği 2015 Nisan ayı seçilmiş ve aynı yılın Eylül ayının son haftasına kadar ölçüm alınmıştır. Aynı zamanda çalışma alanının çevre jeoloji ve hidrojeolojisi araştırılmış, bölgeye ait inceleme ve gözlemler yapılmıştır.

Bu amaç doğrultusunda, maddi imkanları da göz önünde bulundurarak, kaynak değişimlerini daha hassas yakalamak için ölçüm frekansı haftalık olarak belirlenmiş ve seçilen fiziko-kimyasal özellikler toplamda kesintisiz 25 hafta süresince alınmıştır. Ölçüm alınan lokasyonların sayısının ve ölçüm frekansının fazlalığı, ayrıca çok sayıda grafik oluşturmak yerine bir görsel grafik ile sonuca ulaşmak için, metot olarak "matris metodu" seçilmiştir. Bu metot sayesinde deniz ve Azmak ırmağının da bulunduğu 49 noktadan alınan ölçüm değerlerinin 25 haftalık zamansal değişimi sergilenmiştir. Kaynakları tek tek incelemek yerine bir bütün halinde, sistem olarak incelenebilmesini sağlayan bu yöntem, ses mühendisliğindeki spektral analiz yönteminden esinlenilmiş ve bu tezde kaynakların hidrojeolojik yönden incelenmesi için kullanılmıştır.

Oluşturulan görsel matris grafikleri, gözlemin 4. haftasında deniz suyunun ani ısınmasını ve devam eden 5. Ve 6. Haftalarda etkisinin kaynaklarda görüldüğünü göstermektedir. Aynı zamanda Özgül elektriksel iletkenlik değerlerinin ilk haftalarda yüksek değerlerde iken, zamanla son haftalara doğru dalgalanarak azaldığını göstermektedir.

pH değerleri de, muhtemel deniz suyu karışımı sonucu zaman içerisinde belirli bir osilasyon göstererek dalgalanmış ve giderek azalmıştır. pH dalgalanmaların deniz suyunun girişim etkisinin fazla olduğu zamanları gösterdiği düşünülmekte ve o haftalarda karışım suyunun pH değerinin karst suyunun pH değerinden daha az olduğu görülmektedir.

Sonuç olarak, kaynakların su sıcaklığı, özgül elektriksel iletkenlik ve pH matrisleri incelendiğinde, önce deniz suyunda anomali görülmekte, sonra takip eden hafta içerisinde kaynakların pH değerinde, özgül eletriksel iletkenlik ve sıcaklık matrislerindeki değerlerde de anomaller gözlemlenmiştir. Bu durum bu bölgedeki deniz suyu girişminin derin deniz yüzeyinden olmayıp, yüzeye yakın sığ derinliklerden gelen deniz suyu ile meydana geldiğini ortaya koymaktadır.

**Anahtar Kelimeler:** Akyaka, Deniz Suyu Girişimi, Gökova, Karst, Kaynaklar, Matris Metodu, Özgül Elektriksel İletkenlik, pH, Sıcaklık, Türkiye

# ABSTRACT

# A MATRIX APPROACH FOR VISUALISATION
# OF SELECTED PHYSICO-CHEMICAL PROPERTIES
# OF AKYAKA (GÖKOVA) KARST SPRINGS, MUĞLA

Eray AVCI

Master of Science (M.Sc.)

Graduate School of Natural and Applied Sciences

Department of Geological Engineering

Supervisor: Assist. Prof. Dr. Bedri KURTULUŞ

January 2016, 74 pages

This thesis study was completed to contribute and seek answers for the existing seawater intrusion case in coastal karst springs, located in Akyaka district of Muğla, by measuring water temperature, specific electrical conductance and pH values of springs between April and September 2015.

A date to start was defined as the beginning of April 2015 when all springs have high discharge rates and measurements were recorded to the end of September in the same year. Besides, the geology and hydrogeology of the surroundings of the study area were investigated by making in-situ inspections and observations.

On this purpose, also considering the financial sources, the sampling frequency was predefined once a week to catch small changes. The selected physico-chemical features were recorded for a 25 weeks time duration without any interruption. Due to having many sampling locations and high sampling frequency, also to prevent having too many graphs, "the matrix method" was selected to reach the results in one digital image. The 25 weeks temporal change of measurement values of 49 locations, also having values from seawater and Azmak stream, were presented easily owing to this method. This method which gives the opportunity to interpret the whole system as a single body from a larger perspective was inspired from the spectral analysis method in sound engineering and was adopted for hydrogeological analysis of springs in this thesis study.

When the plotted matrice images were analysed, it was clearly observed that the water temperature of springs rose in $5^{th}$ and $6^{th}$ weeks of observation after the seawater had raised rapidly in the $4^{th}$ week of observation. Additionally, specific electrical conductance values showed a decreasing trend by having local fluctuations, although, they were very high in the beginning weeks.

The pH values also had a decreasing trend in time by having oscillations which was probably caused by seawater intrusion. It is thought that those pH oscillations, especially low pH values indicate the times when the seawater intrusion was high in springs. The pH of the mixing water is slightly less than the pH of the karst water.

As a summary, feature anomalies generally observed in seawater at first and then in the following weeks it was observed in springs. It can be concluded that the seawater which involves into the mixing comes from the shallow depths of Gökova Bay not from deep seawater and springs affected from seasonal changes depending on the findings obtained from temperature, specific electrical conductance and pH matrices.

Dedicated to the people who fight for their rights.

# ACKNOWLEDGEMENT

# TABLE OF CONTENTS

# LIST OF TABLES

# LIST OF FIGURES

## SYMBOLS AND ABBREVIATIONS

| | |
|---|---|
| Σ | Sum Symbol |
| **Z** | Matrix Symbol Of A Feature |
| $z_{yx}$ | An Element Of Matrix |
| N | Normality |
| ˚C | Celcius Degree |
| % | Percent sign |
| σ | Specific gravity notation |
| g/L | Gram Per Liter |
| μm | Micrometer |
| m | Meter |
| ml | Mililiter |
| mm | Milimeter |
| km | Kilometer |
| $km^2$ | Square Kilometer |
| $m^3$ | Cubic Meters |
| $m^3/s$ | Cubic Meters Per Second |
| EC | Electrical Conductivity |
| μS/cm | Micro Siemens Centimeter |
| mS/cm | Mili Siemens Centimeter |
| meq/L | Mili Equilivalence Per Liter |
| Log | Logarithm |
| pH | Negative Logarithm Of $[H^+]$ |
| U.S | United States |
| (aq) | Aqua |
| 2-D | Two Dimension |
| 3-D | Three Dimension |
| Na | Sodium |
| Ca | Calcium |

| | |
|---|---|
| Mg | Magnesium |
| K | Potassium |
| CI | Chloride |
| $SO_4$ | Sulphate |
| $CO_3$ | Carbonate |
| $HCO_3$ | Bicarbonate |
| $CO_2$ | Carbon dioxide |
| $N_2$ | Nitrogen |
| $H_2CO_3$ | Carbonic Acid |
| $CaCO_3$ | Calcium Carbonate |
| $H_2O$ | Water |
| $H^+$ | Hydrogen |
| $OH^-$ | Hydroxide |
| $HNO_3$ | Nitric Acid |
| $H_2SO_4$ | Sulphiric Acid |
| KCI | Potassium Chloride |
| HDPE | High Density Polyethylene |
| SpC | Specific Conductance |
| ET | Evapotranspiration |
| PET | Potential Evapotranspiration |
| W-E | West to East |
| USGS | United States Geolological Survey |
| DEM | Digital Elevation Model |
| DSI | General Directorate Of State Hyraulic Works Of Turkey |
| MGM | Turkish State Meteorological Service |
| MTA | General Directorate Of Mineral Research And Exploration |
| ASTER-GDEM | Aster Global Digital Elevation Model |
| dd/mm/yyyy | Day/Month/Year Date format |

# 1. INTRODUCTION

## 1.1. Purpose And Scope

The predefined aim of this thesis study was to observe the temperature, specific conductance and pH values of Akyaka springs weekly in a time period of seven months and finally to classify the springs by applying a visual method, 'the matrix method'. Beside this, the main target is to seek new scientific clues and evidences to define the predominant process which is responsible for the seawater intrusion in this coastal area and to contribute the initial studies.

## 1.2. Literature Review

Water, the most precious and vital natural source on Earth, does not get its real value from people who also contains water almost three of four in their body mass and use it every day to maintain their lives and health. It has been known that the access to clean and usable water is getting harder lately due to rising human population and water demand as well. Global warming and climate change also affect regional and local rain precipitation regime and so does groundwater systems.

From the ancient times to present, at different places on Earth people use springs for their fresh water needs (Kresic and Stevanovic, 2009). When we classify springs according to their discharge rates, it is noticed that most of the springs, which are used by people, come out from karst structures. These type of rock mass units may have very large, macro-scale dissolution voids and cavities which were caused by chemical reactions occurred in carbonate rocks that are very soluble in acidic aquatic environments.

In Turkey, there are many karst areas. The most famous area which has thousands of springs in its structure is known as Taurus Mountain Belt orientated West to East just

parallel to the Mediterranean Sea in the south part of Turkey. Highly karstified limestone and dolomite units supply water for human needs and irrigational usage. The 'Dumanlı Spring', one of the biggest karstic springs in the world with its 50 m$^3$/s discharge rate, is located in Taurus Mountains in Turkey (Kresic and Stevanovic 2009).

The west edge of that karstic zone also exists in Muğla province of Turkey, which this thesis project area is also located. It has lots of karstic structures and springs. Most of the springs are located on the border zone with neigbourhood province Antalya. Rest of the springs shows distributed pattern controlled by geologic and tectonic processes all over the province. Those springs are either geothermal springs or fault controlled shallow to deep karstic springs.

The Gökova karst springs zone is a group of springs which are located in Gökova bay near Akyaka village. The initial hydrogeological studies which were conducted on this area started in 1992 by General Directorate of State Hyraulic Works of Turkey (DSI). Later on, Kurttaş (1997) studied this coastal spring system in terms of environmental isotopic compositions and about the origin of possible recharge zones. Kurttaş and Bayarı (1999) examined salinization effect on this aquifer system. Açıkel (2012) studied Gökova Karst springs on a regional scale and built a conceptual hydrogeological model up for the related area, moreover the possibility of venturi effect for seawater intrusion was mentioned.

The studies based on physico-chemical properties of spring water, especially on water temperature and electrical condutivity changes, were started in the United States. Manga (1998) studied on cold water springs in Oregon Cascades area and recorded water temperature values. He calculated the surface water heat flux depending on temperatures and made a comparison with the calculated heat flux of regional deep groundwater circulation. Later on, Manga (2002) expressed that the water temperature of springs could be valuable data when determining the direction of the convectional heat transfer in reservoirs. Moreover, it was stated that the water temperature is a good tracer to use for groundwater systems (Anderson, 2005).

Baena et al. (2009) recorded periodically water temperature and electrical conductivity values of karstic springs located on the Sierra De Las Nieves karst aquifer in Spain to understand the internal dynamics of the system. As a result, it was

concluded that water temperature and electrical conductivity values must be evaluated together. Secondly, it was stated that electrical conductivity gives fast responses to changes. However, temperature values, when making a judgement about the whole system, can be preferred due to slow response of the rock mass that in heat equilibrium.

There is also flow model studies using groundwater temperatures such as the case study of Long and Gilcrease (2009). In this study, a one dimension grounwater flow model is constructed and, according to theoretical results and real conditions, the groundwater velocity and mass transport rates were calculated. It shows that the water temperature values are also very impotant for groundwater model calibrations.

Luhman et al. (2011) clearly got results from his study on 25 karstic springs in southeast Minnesota. Springs were classified into two groups which were affected from precipitation and those which were not. By using the the affected group, it was found that some thermal change pulses were caused by precipitation. So, it was concluded that the aquifer size and geometry can be estimated from this temperature approach. Luhman et al. (2012) also studied on a karstic system and used a tracer then compared it with temperature model.

On the other hand, the salinization of coastal aquifer systems is a common environmental problem among the mediterranean countries.

Custodio et al. (1987) carried on a study in coastal carbonate formations in Catalonia, Spain and made observations in wells which were salt polluted and had brackish water due to existence of a very permeable carbonate aquifer. They examined the geochemical parameters of mixing water in wells. The interesting point from this study was the pH change of the fresh, brackish and the seawater samples from different zones.

Smart et al. (1988) also stated another useful information which is mixing-induced carbonate dissolution in the mix water in limestone aquifers. Thus, caves can be formed in respect with increasing carbon dioxide and ionic activity.

Duriez et al. (2007) examined thermal springs and their water chemistry which has different seawater contamination rates and also observed carbondioxide degassing at outlet points and a slight pH drop lower than the calculated value in springs.

# 2. PROJECT SITE

## 2.1. The Project Site

The study area is located at southwest part of Turkey in Muğla province near a small touristic village known as 'Akyaka' village.



**Figure 2.1. The study area location on Turkey map.**
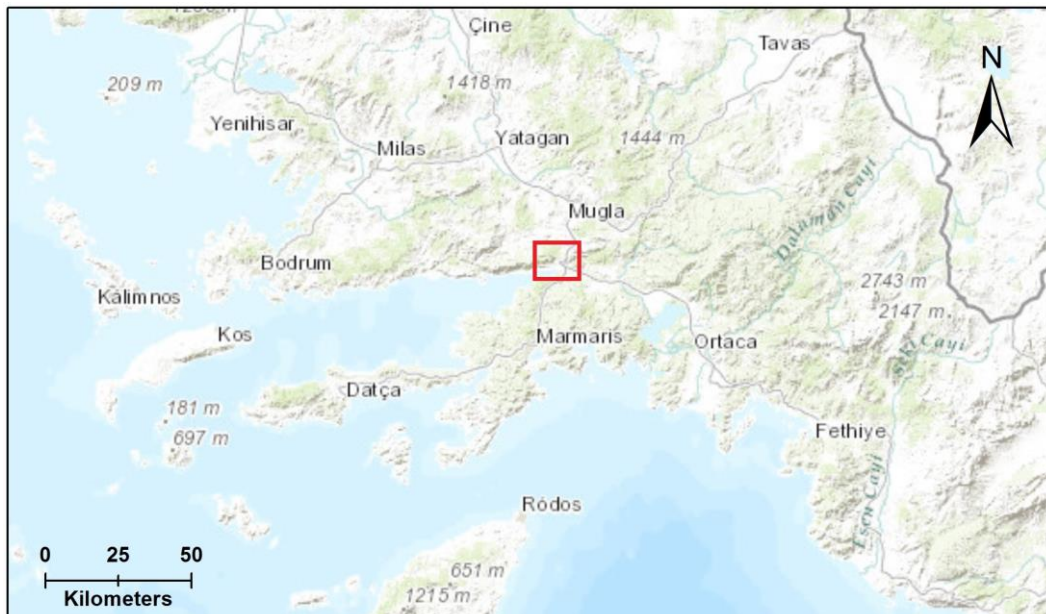


**Figure 2.2. The study area location in Muğla province in Turkey.**

4

In this study area, the main observation work was conducted on a line of karst spring outlets, which are located at approximately 1 km southeast of Akyaka village in Muğla province in Turkey.
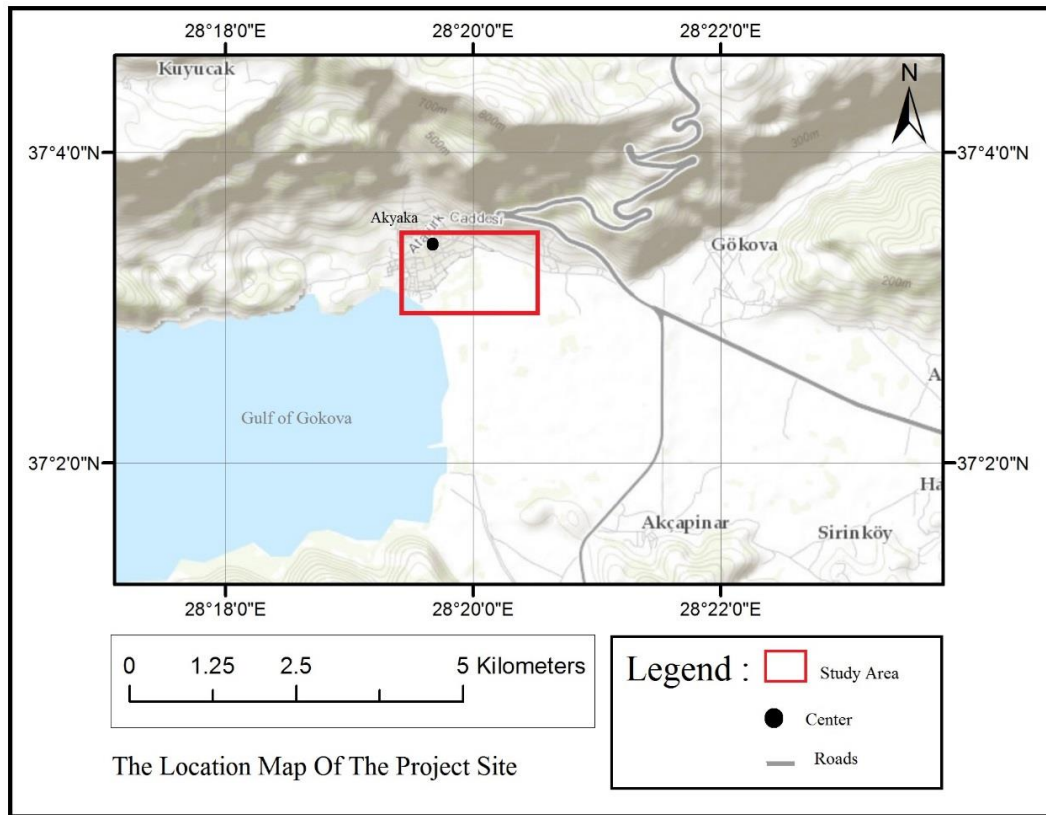


**Figure 2.3. The precise location map of the project site.**
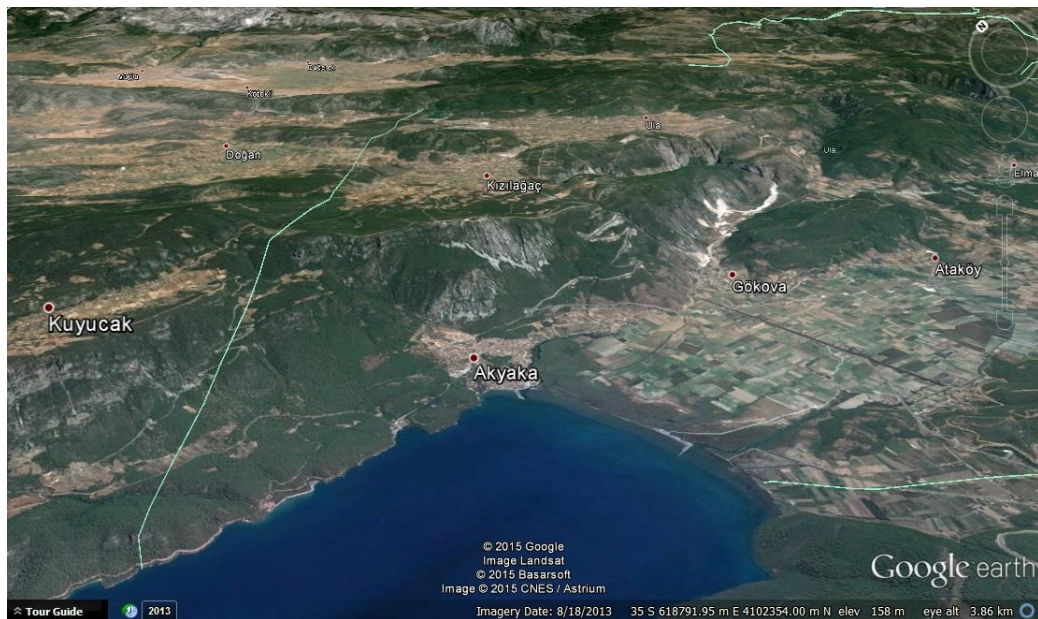


**Figure 2.4. The 3D Google Earth view of the study area.**

**Figure 2.5. A general view of Akyaka village from Mount Sakar.**



**Figure 2.6. Akyaka village sea level point.**

## 2.2. Geography

Muğla province, which also has the same name with its capital city, is located at south western part of Turkey where two seas, the Aegean and the Mediterranean Sea, meet with each other in the Gulf of Gökova. It has hot and arid Mediterranean climate conditions, however in winter it has a warm, slightly cold weather and gets heavy rains due to its dramatically changing physical relief pattern (Ertürk and Atasoy, 2010). The altitudes as high as 2296 meters (Mount Sandras) existed at inner areas in the province. According to Turkish State Meteorological Service (MGM) the long term (30 years) annual mean temperature is 16.15 ˚C degrees for the capital city of the province which is at 650 meters above from the sea level. The long term (1950-2014) summer mean temperature is 25.1 ˚C degrees and the winter mean temperature is 6.2 ˚C degrees, annual mean temperature is 15.05 ˚C degrees for the whole province (Ertürk and Atasoy, 2010). The annual mean precipitation is 1159.2 mm as well for the 64 years period for this province (Anonymous, MGM, 2015).
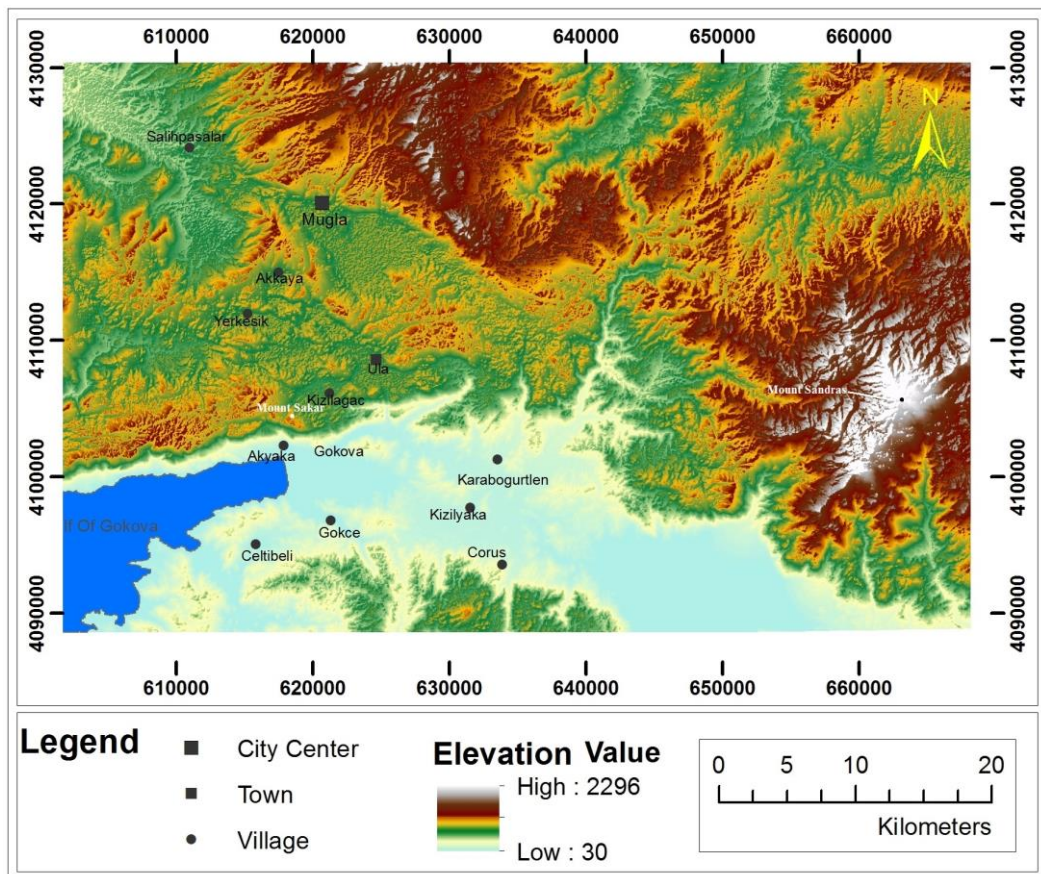


**Figure 2.7. The physical map of Muğla province.**

7

The study area in Akyaka village is on Gökova bay which was formed by a rifting effect of an young extensional fault system. Here the altitudes, due to natural relief, reaches 0 to 900 meters in a 2 km distance. The 'Mount Sakar' or 'Sakar Pass' (897m) is the highest point just behind the study area.

Therefore most of the precipitation falls down directly to that mount at first touch of the clouds. Furthermore, the east part of this bay leads clouds to inner area to a small town named 'Ula', a small town which gets the highest amount of precipitation in the whole province. It is also one of the areas that has high annual precipitation rate in Turkey (See Figure 2.19.).

## 2.3. Geology

## 2.3.1. Regional geology

Due to its geographical and geological location between Eurasian, Pan-African and Arabian plates, Turkey has a very complicated multi-phased geological evolution history comparing to other inner continental areas. As Ketin (1983) stated in his book, Turkey started its geologic life in Paleo-tethys Ocean in late Paleozoic era and having rifting and ocean closing mechanisms in Mesozoic. Finally Turkey rose up over to the sea level completely in Miocene epoch due to Alpine orogenesis. Turkey also had local volcanism and large tectonic movements in this upper Cenozoic Era.

The south-west of Turkey, where the project site of this thesis study is located (Muğla province), has 3 main geological mass units underling other young units. (See Figure 2.8. modified from Koralay et al. (2011).)

1) The Menderes Massif

2) The Lycian Nappes

3) The Beydağları Autochthonous Unit
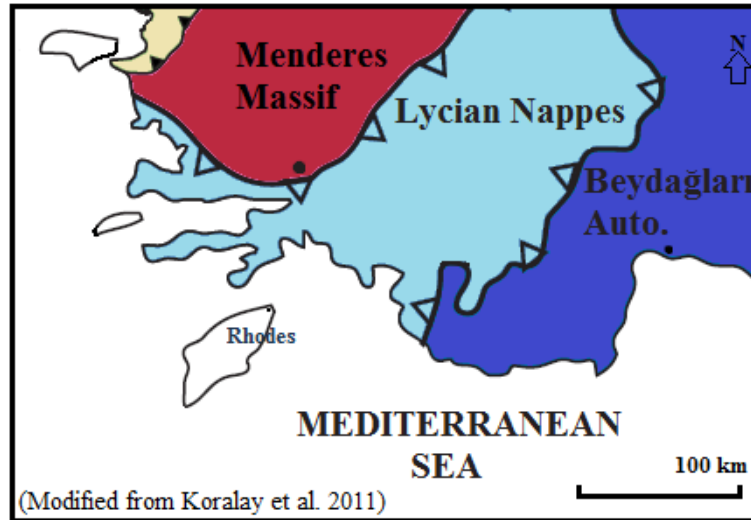
**Figure 2.8. Simplified geological setting of southwest Turkey.**

The first unit is known as "Menderes Massif", the metamorphic unit, which has two different group of layers "Pan-African basement" and cover units. The Precambrian-Cambrian aged Pan-African basement unit is orthogneiss and the cover units are Paleozoic 1) micaschist 2) phyllite-marble envelope units and 3) Mesozoic to Cenozoic marbles.

The second geologic mass unit is Lycian Nappes which tectonically overlapped Menderes Massif cover units near Ula-Gökova region (Graciansky, 1972). This nappe package is thought that it was transported from North to South over the Menderes Massif between Mesozoic and Cenozoic Eras (Graciansky, 1972; Dürr, 1975; Dürr et al. 1978; Gutnic et al. 1979; Şengör and Yılmaz, 1981; Okay, 1989; Collins and Roberson, 1997, Collins and Roberson, 1998, Collins and Roberson, 1999; Rimmele et al. 2003). Lycian nappes are a composition of three units also. From top to bottom , Lycian Ophiolites-Peridotites, a mixed melange unit and thrust sheet sediments (Collins and Robertson, 1997; Rimmele et al. 2003 ). The ophiolite nappe is a mix of peridotites, dunites, harzburgites and Serpentines. Beneath this crustal pieces, there are limestone (dolomite in some places) formations came from the Anatolide zone.

The last geologic mass unit tectonically contact with Lycian Nappes is Beydağları Autochthonous unit near Antalya-Muğla province border. This Cenomanian-Early

Miocene carbonate mass unit is formed from thinly bedded micritic limestones and thickly bedded calcarenites (Graciansky, 1968, 1972; Bayarı et al. 1995).

Although, this unit's surface expositions are not seen near the study area, it is thought that the tauride tectonic unit may be the basement rock under Lycian Nappes. Beside this, due to its tectonic role in the past geologic time, it is necessary to mention it here to complete the big geological picture of this region (See figure 2.8.).

After the Lycian Nappes had travelled to the south during Early Miocene time, they emplaced onto the Antalya basin until late Miocene time (Robertson, 2000; Gürer and Yılmaz, 2002). It is also thought that the Miocene extentional tectonic movements in Southwest Turkey formed the last morpho-geological setting of this Nappe settlements. Moreover, during that geologic time periode W-E extentional tectonic movements built up Milas-Ören and Muğla-Yatağan grabens. The N-S extentional movement, which had started during late Miocene time, started to form N-S trending grabens, including Gökova Graben (Graciansky, 1972; Gürer and Yılmaz, 2002). Later on, those and surrounding depression areas then were filled by fluvial Pliocene marl, conglomerate, limestone layers and marine deposits at some places.

Finally, W-E trending normal fault system started at a regionwide scale on the Northern side of Gökova Gulf by cutting the Neogene sediments and the Lycian Nappes. Even though the age of the W-E fault mechanism on the Northern side is not clear, the current study of Gürer and Yılmaz (2002) gives Quaternary age to that fault system.
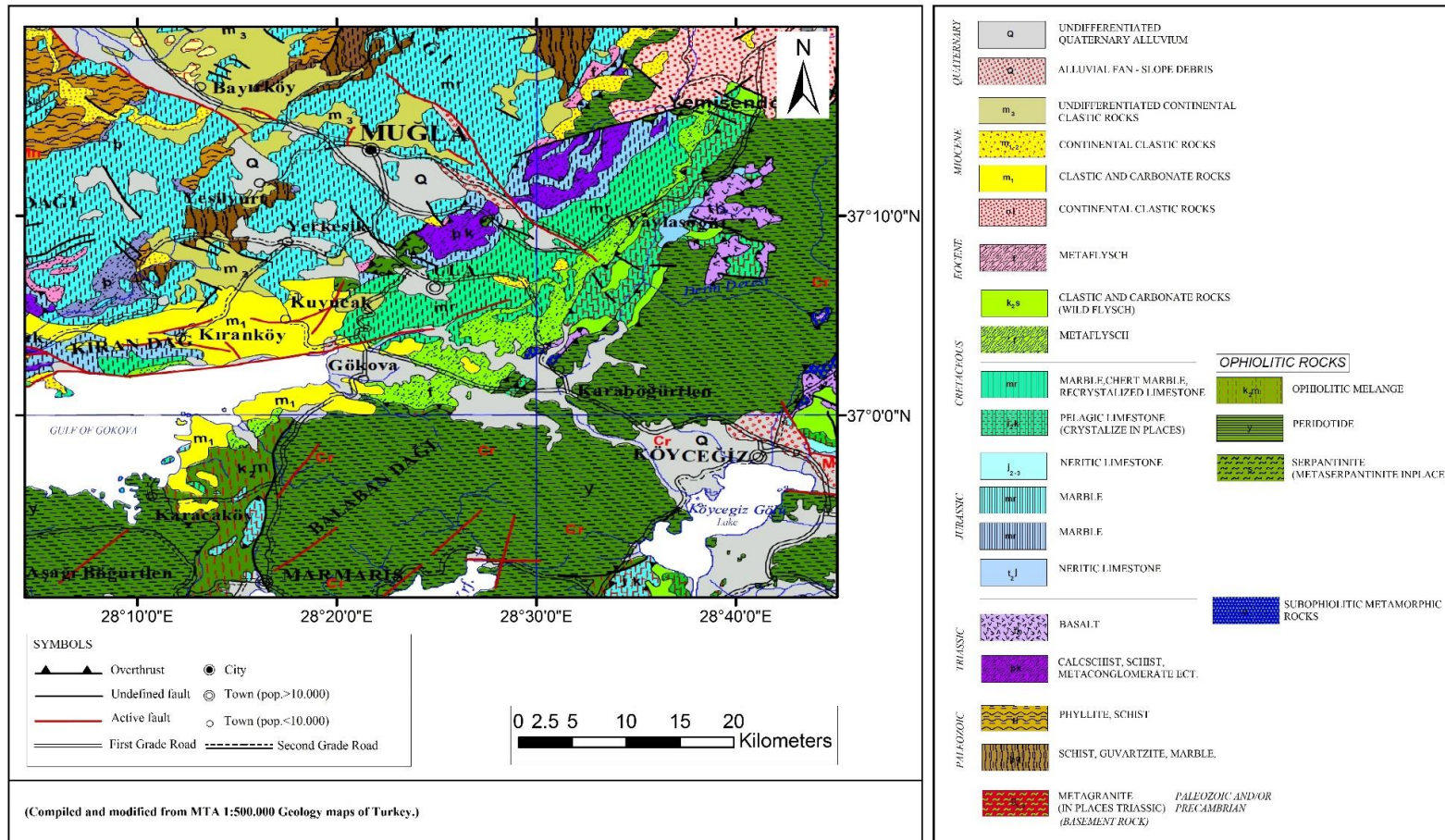
**Figure 2.9. The detailed geological map of Muğla region.**

11

## 2.3.2. Local geology

The detailed geological information for the study area was obtained from the (parcel number: Aydın-N20c4) MTA 1:25.000 geology map and a new geology map was drawn with a few additional geological features depending on field trip findings.

Akyaka karst springs are on the contact of slope debris and Quaternary alluvium. Springs directly discharge into the open channel of Azmak stream. In the study area, due to geomorphology it can be observed tree geological units. Mainly Slope debris and Alluvium, but at higher altitudes in the north the early and late Miocene carbonated clastics, conglomerates interbedded with sandstones also exist. This Miocene formations overlie Cretaceous limestone unit which is seen as a high mountain (Mount Sakar - See Figure 2.6., Figure 2.7.) in the northeast of Akyaka village.
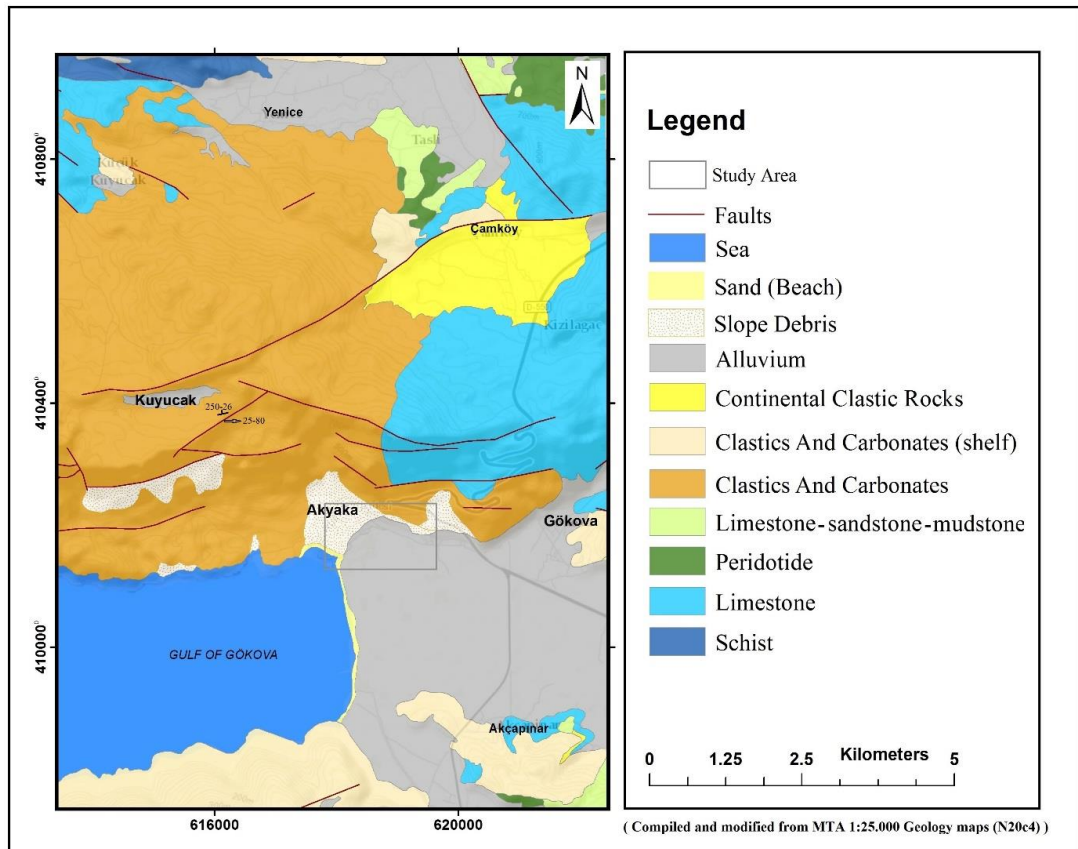


**Figure 2.10. The geology map of the study area and its surroundings.**

The youngest geological unit in the study area is Quaternary alluvium which was deposited in Gökova lowland. According to preliminary geoelectrical studies carried out on the whole lowland area, the unit is not homogeneous and has a listric fault dipping from the south to the North (Çağlar and Duvarcı, 2001). It also mentioned that the rifting movement of Gökova graben system ends in the East part due to the shallow geoelectrical basement profile. In the Northern part there is also a burried fault zone which is oriented West to East (Çağlar and Duvarcı, 2001).

The Azmak Stream seperates the alluvium unit and slope debris which is consist of debris material and loose reddish soil on top. Even though it seems as all springs come up from the slope debris unit, it was observed that some of the springs comes upward from the bottom to the top of the Azmak stream channel. Because of a human effect, a fill road, some springs seems like they come out from the Slope debris. This artificial effect was shown in the discussion chapter. (See Section 6. Page 61)

The Miocene fluvial clastics and carbonates were overlained by slope debris. This unit mostly consist of fluvial clastics and conglomerates, sandstones in places, some are fully filled with carbonate matrixes (Figure 2.11.).



**Figure 2.11. The Miocene conglomerate and sandstone.**

Under those Miocene units the Mesozoic limestone units lied and formed a basement rock mass. This units are Cretaceous Marble-limestone and tectonically subducted Jurassic Marble-limestone unit near Muğla city center (See Figure 2.9.). These Mesozoic Marble-limestone units has a very large area coverage in Muğla province.

There are also some Allochtonous Triassic schist mass packs and Cretaceous peridotite mass packs in some places in the surroundings of the study area which were transported due to the tectonic nappe movements.

The surroundings of the study area also examined through the perspective of tectonism, as it seen in the geologic map there are fault systems mostly on the North and Northwestern side of the study area. These faults are vertical block falls and normal fault systems with very high dip values. They built deep valleys, however due to the dense vegetation it is very hard to detect fault and layer outcrops. Some fault and layer outcrops was detected during the field trip. In the hydrogeology section, it was also given more detail about those structures.



**Figure 2.12. A fault outcrop from the northwest of the study area, on Kuyucak village road.**

## 2.4. Hydrology

### 2.4.1. General hydrology of study area

To present the current hydrological basin and watershed structure of the surrounding area of the study area, primarily a free digital elevation model (DEM) map was taken from the web-site of USGS in suitable size including surrounding basins.

The DEM map has a 1 arc second, 30 meters grid of elevation postings in ASTER GDEM GeoTIFF format signed 16 bits. It has the WGS84/EGM96 geoid system. The given accuracy for vertical data is 20 meters at 95 % confidence. For horizontal data it is 30 meters at 95 % confidence ( http://gdex.cr.usgs.gov/gdex/ , Anonymous, 2015).

Hydrological basin maps showing stream network and watersheds were generated from DEM map by using ArcGIS software. The WGS84 and UTM zone 35S were selected as a geodetic datum and spatial reference for this area. Some necessary adjustments were also applied such as the critical "Fill" adjustment for DEM map, although there are sinkholes in drainage basin areas. Their cell locations were known and cell data were checked to prevent the occurrence of wrong stream paths.

The stream network was generated to show main stream paths which have an accumulation flow greater than 5000 cells for regional scale and 500 cells for more local scale.

Additionally, watershed boundaries were reshaped and adjusted for some locations due to human effects (roads, catchments), geological conditions and groundwater flow direction. The groundwater flow which comes from Gökova lowland towards the biggest spring is known from Açıkel (2012). However, since the springs were stated as karst springs (Kurttaş, 1997; Açıkel, 2012), the surface drainage area for the springs was defined and adjusted according to the contribution priority of the Ula sub-basin.

All meteorological information (except maps: Figure 2.13, Figure 2.14. and Figure 2.15) in this chapter was taken from Turkish State Meteorological Service (MGM). (http://www.mgm.gov.tr/ , Anonymous, 2015).
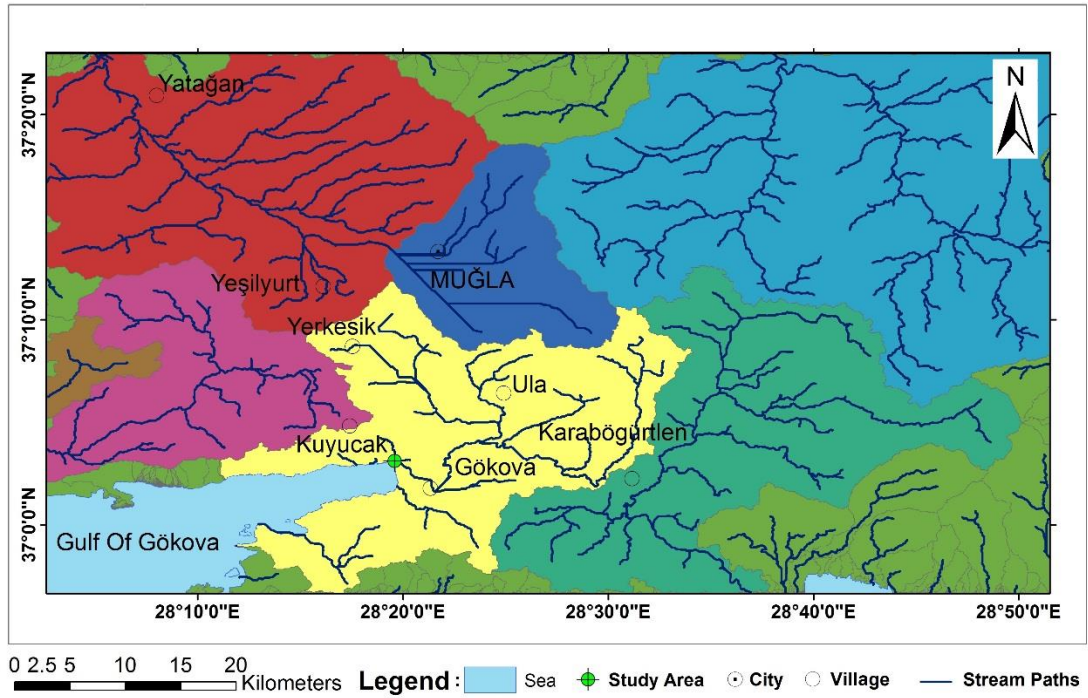
**Figure 2.13. The water basins and general stream networks of Muğla province.**
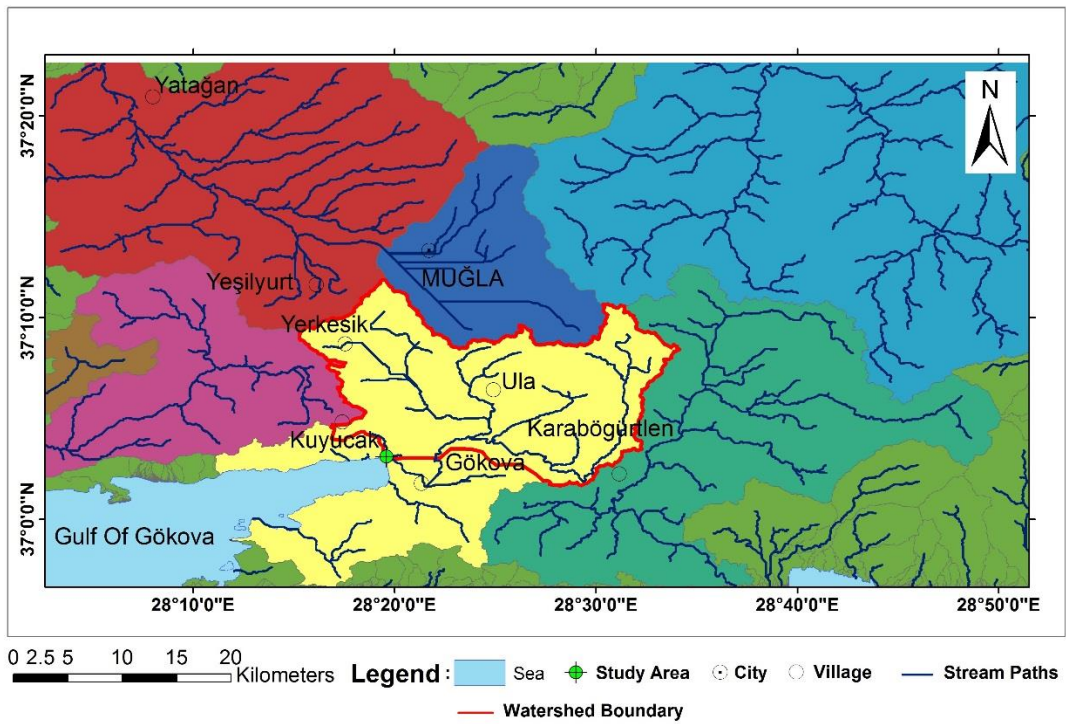


**Figure 2.14. The Gökova basin and the watershed for Ula sub-basin.**

16

The watershed of the surrounding area of the study area is indicated with red colour lines (Figure 2.14.). In this Gökova basin, the total water basin area does not match with the watershed area of springs because there are tree sub-basins. One of them is a small slope area in the west and the other is located in the southern part of the basin where the topographical inclination changes direction. The yellow areas which locate outside of the watershed boundary represent the areas that pour their water outside of the Ula sub-basin (Figure 2.14.).

The calculated drainage area for springs' basin, the Ula sub-basin, is 286 km$^2$.
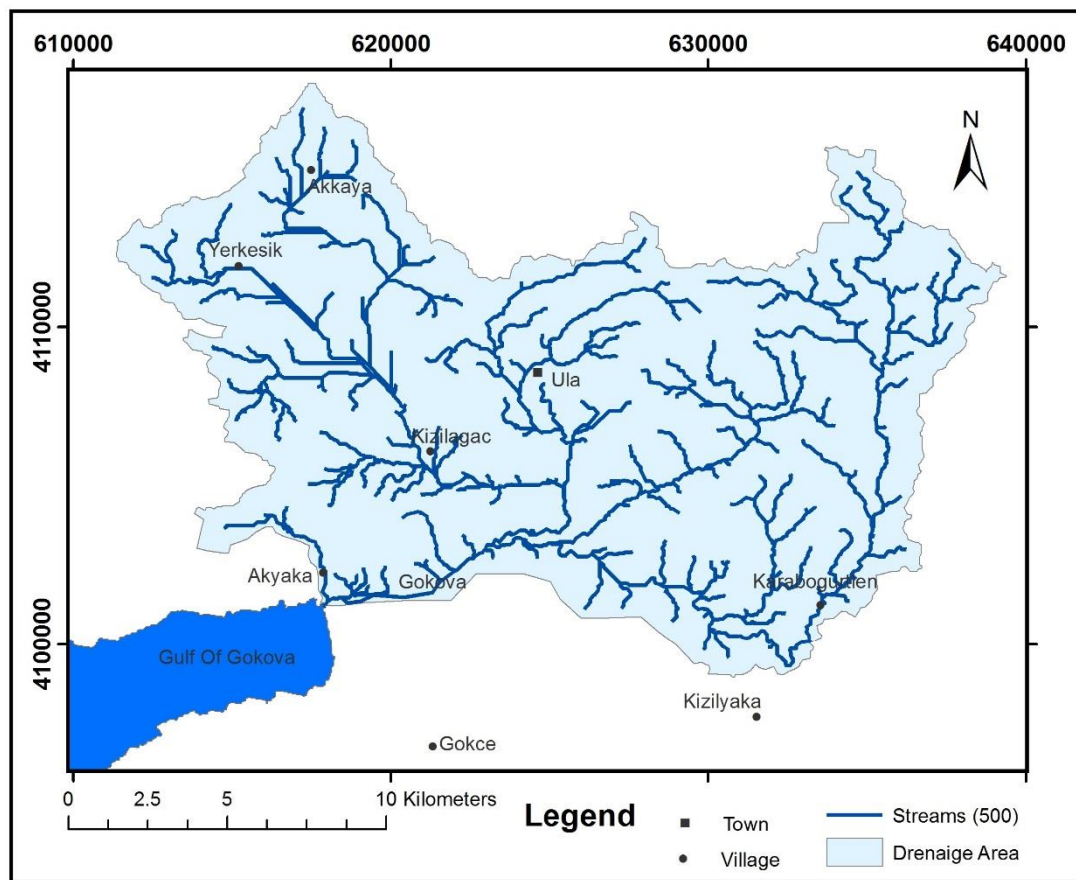


**Figure 2.15. The detailed drainage area (Ula sub-basin) of Gökova karst springs.**

Even though the stream network has such a dendritical water catchment structure, these network is mostly dry in a year time. Since the geological setting consist of slightly metamorphised karstic limestones (Mezosoic marbles) and Quaternary alluvium plains on them, streams disappears in those alluvial plains. In the winter, those plains are flooded. There are also numerous sink holes all over the countryside.

17

As stated before in geography section, the long term (1950-2014) summer mean temperature is 25.1 ˚C degrees and the winter mean temperature is 6.2 ˚C degrees, annual mean temperature is 15.05 ˚C degrees for the whole province (Ertürk and Atasoy, 2010). The annual mean precipitation is 1159.2 mm for the 64 years period for this province (Anonymous, MGM, 2015).

The climate diagram (Figure 2.16.) was made using the data which was taken from the web-site of MGM.
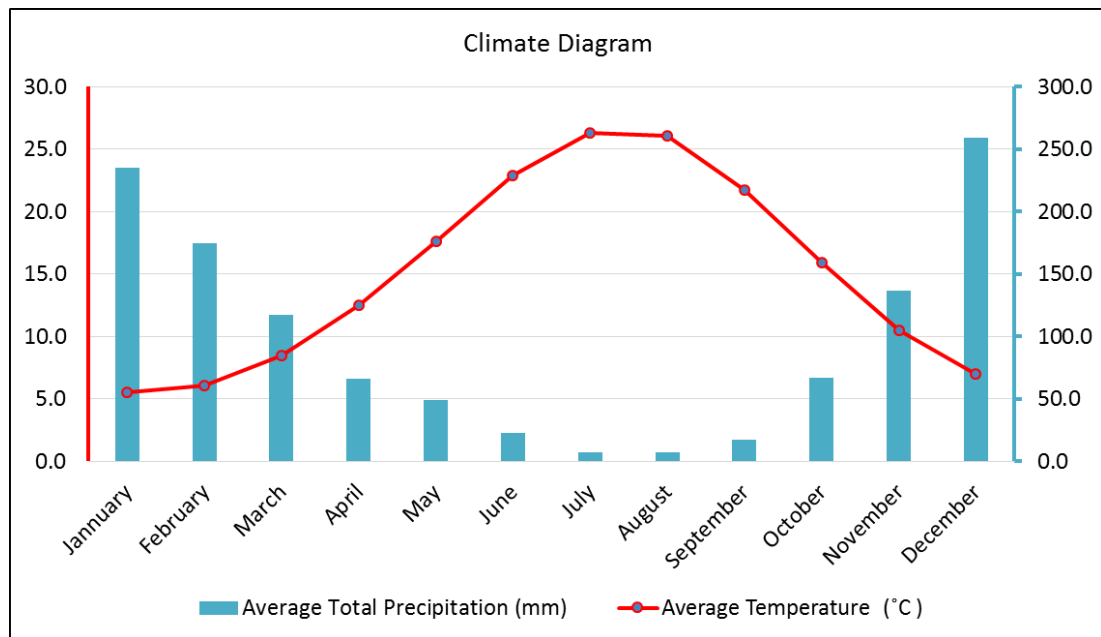


**Figure 2.16. The climate diagram of Muğla.**

According to climate diagram of Muğla (Figure 2.16.) and Thornthwaite climate classification of MGM in their web-site, the climate of this region can be described as humid climate with an evaporation rate of 54% in summer months (Anonymous, MGM). Typical mediterranean climate reigns in this region.

In summer months, it is known that the municipality of Ula supply water from Akyaka springs for the residents of Akyaka (Anonymous, Public Report, 2015). The pumping station is located near the spring which has the lowest specific electrical conductance value.

As it shown in figure 2.16., hot and arid summers are seen in a region wide scale. In alluvium plains, karst poljes, evaporation rate is really high and noticeable to eye in rainy seasons (Figure 2.17.).



**Figure 2.17. A view from Muğla polje showing visual evaporation in April 2015.**
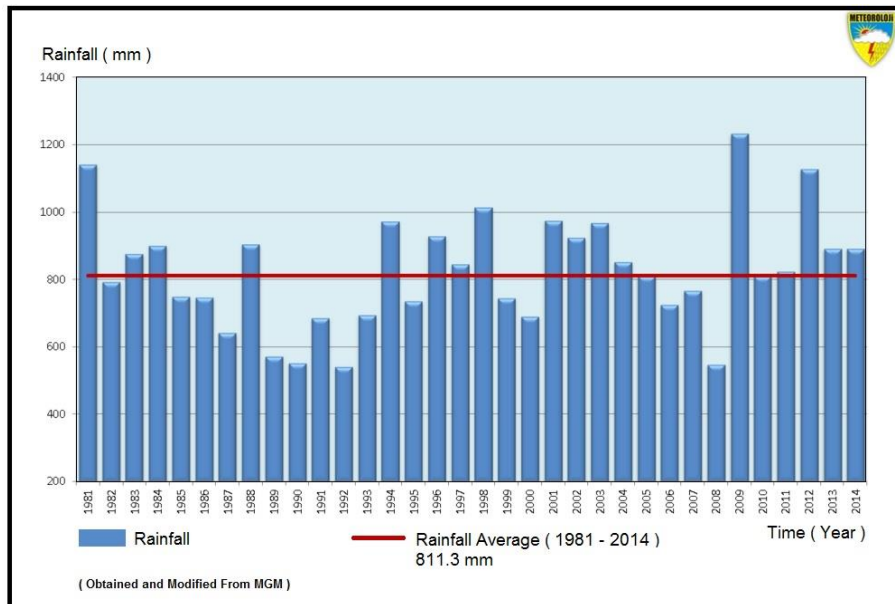


**Figure 2.18. The rainfall precipitation graphic of Muğla.**

It is indicated that the long term average rainfall precipitation is 811.3 mm. This precipitation value gets higher about 1000 mm in Ula sub-basin of Muğla region (Figure 2.18. Figure 2.19. and Figure 2.20. were taken and modified from MGM).
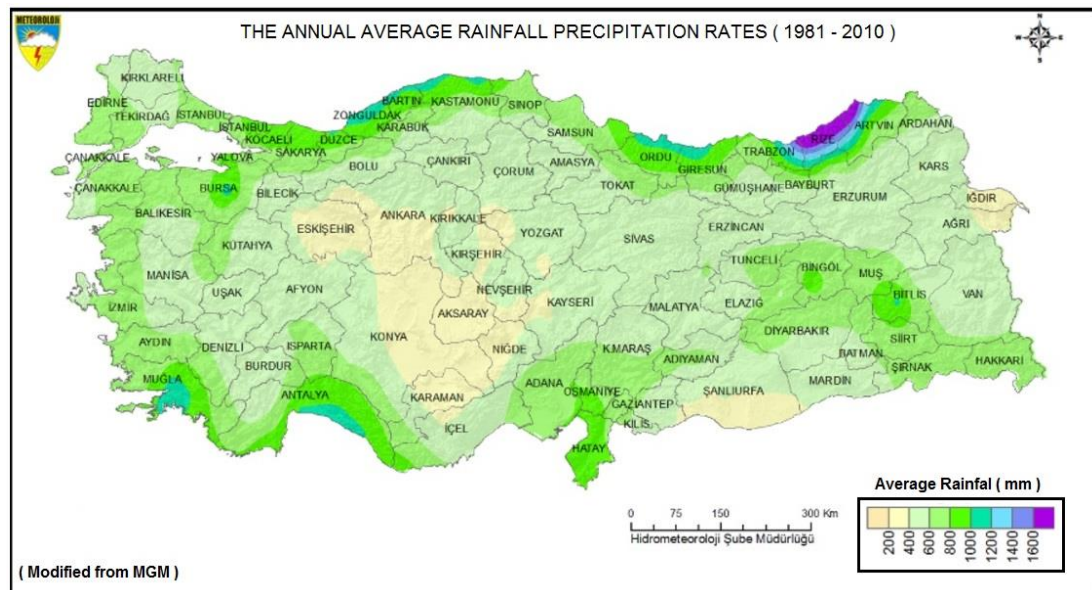


**Figure 2.19. The average rainfall rates of Turkey ( 1981 – 2010 ).**
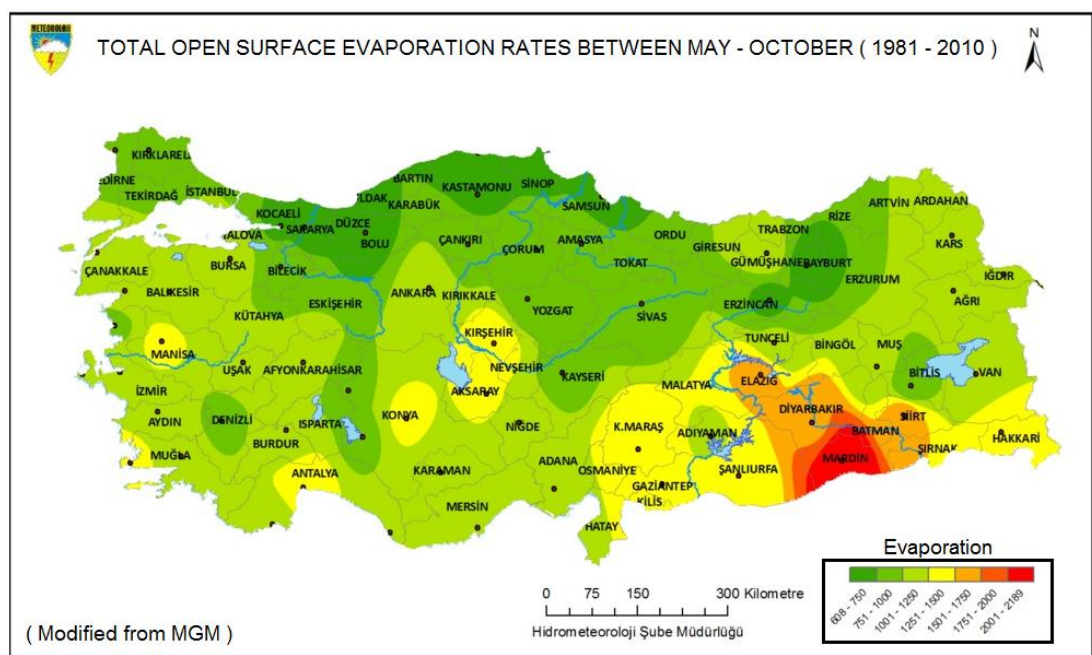


**Figure 2.20. The open surface evaporation map of Turkey.**

The Thorthwaite-Matter evapotransporation method was thought to be applied for this basin because of the minimum data requirements. On the other hand, since this region is a karst region of Mesozoic limestones having different karstic structures

such as Polje plains , sink holes and high evaporation rates, water does not reside long enough in soil zone in some places. Furthermore, in the winter in local Poljes some flooded areas are seen as small ponds of which are needs open surface evaporation methods to estimate the real evaporation amounts.

Thorthwaite (1948) also questioned his work. He exactly wrote : " *The mathematical development is far from satisfactory. It is emprical.*" He also mentioned that the potential evapotranspiration ( PET ) related to a given temperature is different for different places (Ward and Trimble, 2003). Jensen et al. (1990) stated that Thornthwaite's method is suitable for the areas which has similar climates like the central east U.S (Ward and Trimble, 2003).

Additionaly, According to Peel et al. (2007), updated the Köppen − Geiger climate classification, central U.S. has a temperate climate which gets rainfall in the two half of the year. Conversely, the study area is located in Mediterranean climate which gets rainfall only in the winter and has arid hot summers.

In the light of these local (field observations) and literature information, the applicability of Thorthwaite-Matter's ET calculation for this region was questioned and it was withdrawn from this method.

From the preliminary studies, Kurttaş (1997) applied different ET Methods for this region. It was estimated tree evapotranspiration values by applying the TURC , the Temperature - Altitude Relationship and the conservative Chlorine ( CI ) method.

As he stated in his study, the tree methods gave close values to each other. The final calculated theoretical ET for the specified region was the 50% of the total rain precipitation.

In this conditions, a theoretical annual groundwater recharge for the Ula sub-basin coming just from the rain precipitation can be given as 116.015.900 m$^3$ , when the average rainfall is 811.30 mm and 50% of the rain precipitation evapotranspirates on a drainage area of 286 km$^2$. This average recharge value was just calculated and was given here to give an opinion about the mean groundwater recharge of the related sub-basin which probably feeds Akyaka karst springs. It is also suspected that springs are fed by other neigbourhood basins (Kurttaş 1997; Açıkel 2012).

## 2.5. Hydrogeology

## 2.5.1. Regional hydrogeology

Hydrogeological studies about Gökova Akyaka springs in Muğla region are very limited. DSİ unpublished research reports can be accepted as initial hydrogeological studies. The following studies are exist in chronological order, Eroskay et al. (1992) unpublished, Kurttaş (1997), Açıkel (2012). Kurttaş (1997) studied the isotopic compositions and the physico-chemical properties of karst springs along the coast line starting from Akyaka to Ören village. The geological distributions of hydrogeological units and possible recharge areas were given. Also a hydrogeologic budget was calculated. The seawater intrusion was mentioned and seawater mixing percentages was calculated. Açıkel (2012) recalculated the water budget and gave a new conceptual hydrogeological model for Akyaka karst springs.

Due to rapidly changing technological conditions and to contribute the initial works, it has been decided that it could be beneficial to redraw and present hydrogeological maps of Muğla region and the surrounding area of the study area in a different perspective of scientific view.

While it had been prepairing, the MTA 1:500.000 geological map of Denizli – Turkey (Konak and Şenel, 2002) was used as a reference base map for hydrogeological feature map of Muğla region. For local hydrogeological feature map, the MTA 1:25.000 geological map of Aydın (N20c4) parcel selected as a reference base map.

The prepared regional scale hydrogeological feature map shows geological units which can be classified as aquifers and which can be classified as non-aquifers in Muğla region (See figure 2.21.). Likewise, the local hydrogeological feature map shows the same hydrogeological properties of rock units (See figure 2.23.).

The colour references were taken from " *International Legend For Hydrogeological Maps"* (UNESCO, 1983). Revised version.

The hydrogeologic feature map below, which covers approximately 3000 km$^2$ land surface, presents geological units which are classified as aquifers and non-aquifers.
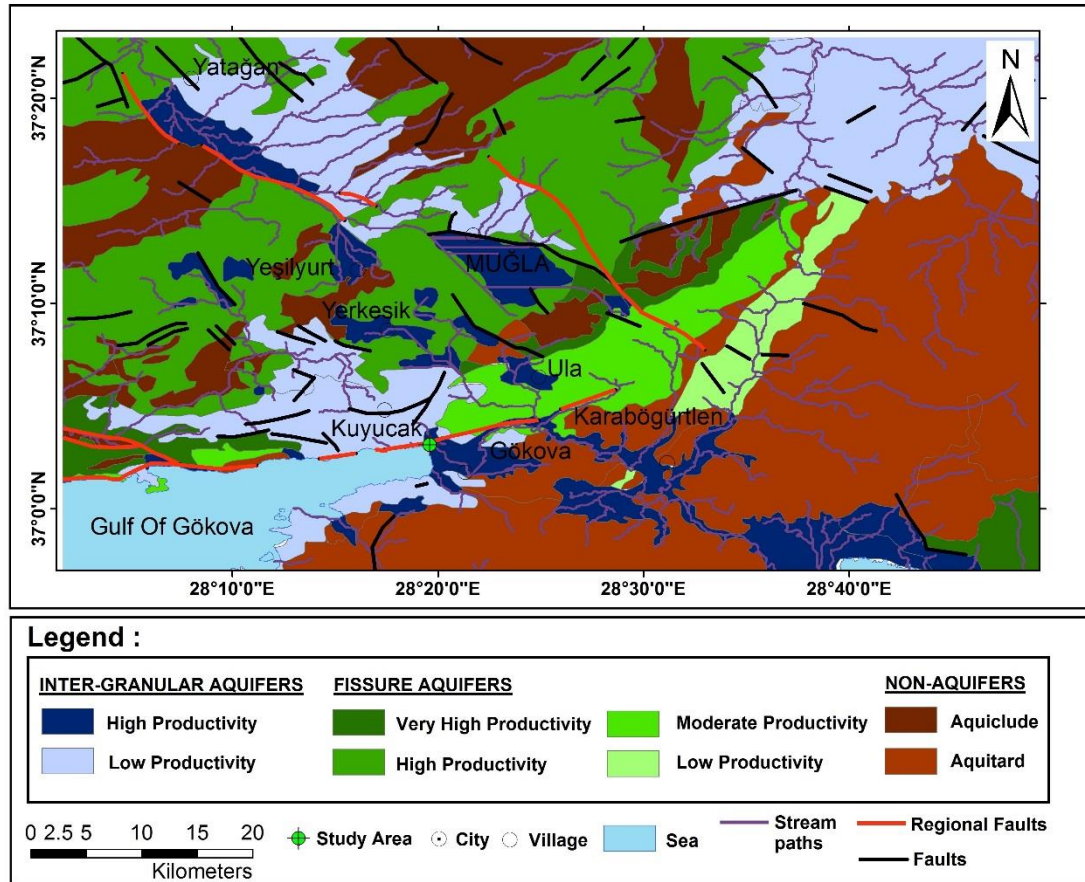


**Figure 2.21. The regional hydrogeological feature map of Muğla region.**

In this map (Figure 2.21.), semi-metamorphised limestone units, karstified marbles, were shown in green tones and pelagic limestones were coloured in pale-light green tone. Alluvium units in plains, lowlands and also slope debris masses in valleys were coloured in dark blue colour.

Lithified sedimentary units of which are generally fluvial deposits and clastic carbonates were coloured in light grayish blue colour. For non-aquifer units such as aquicludes and aquitards the brown colour were used. Light brown colour was used for fractured peridotite and flisch units as aquitards, dark brown colour was used for phyllite – quvarsite and schist units as aquiclude units.

Regional faults were presented with lines in red colour while the small scale faults were shown with black lines.

23

Stream paths were also added to give an idea about the current surface drainage area conditions.
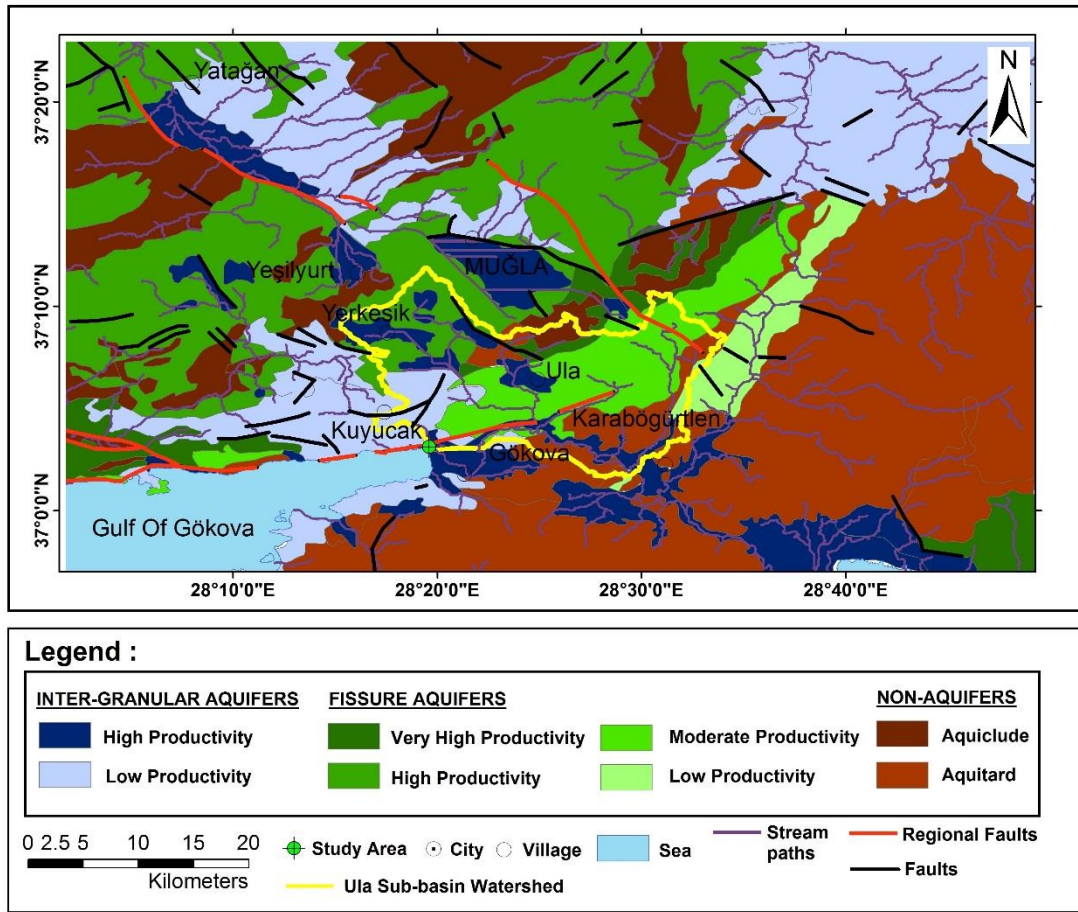


**Figure 2.22. The regional hydrogeological feature map of Muğla region and Ula sub-basin watershed.**

As it seen in the map, the surface drainage area lies on a very large fissured and karstified limestone (marble) area. Sub-surface groundwater connections are strongly possible due to the geological and tectonic setting of the area.

Fault systems, especially regional fault systems play a critical role on groundwater movement in the karst areas in Turkey (Kresic, Stevanovic 2009). As it was stated, in karst areas which were metamorphised, especially fault planes become good paths for groundwater movement, instead of dissolution structures such as caves and voids.

There are also possible groundwater input and output locations between the basins surrounding the Ula-subbasin. In the discussion section they were pointed out. (See Figure 6.1. page 56.).

## 2.5.2 Local hydrogeology

In a local scale, mostly considering study area and its surrounding area, a hydrogeological map was prepared to indicate the units which are considered as aquifer units depending on their geological properties.
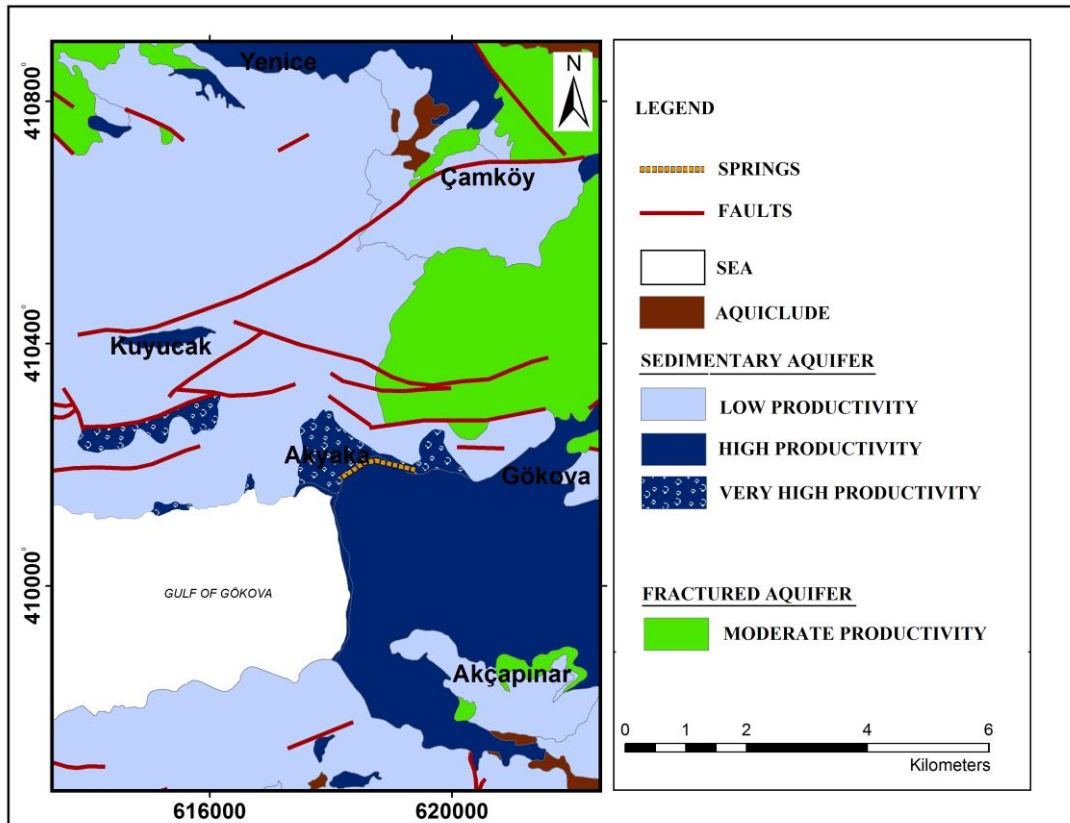


**Figure 2.23. The local hydrogeological feature map of geological units.**

As it had been mentioned and showed before in initial studies, especially in Kurttaş (1997), the area in the north and north-east, taking the springs as a refence point, has lots of tectonic structures such as micro and macro scale normal and vertical faults.

In this section most of the geological units which were visited and observed in field trips were explained in respect of hydrogeological perspective. It is also observed that some faults and layers give outcrops on some locations.

Having explained the geological unit properties before, several units around the study area were presented in this section by starting from the closest geological unit slope debris (See Figure 2.24. Figure 2.25.). The areas in dark blue with white dots in the local hydrogeological map (Figure 2.23.) represents this slope debris unit.

25

The weathering effect on the units of this area is really visible physically. Debris masses overlie and cover gradually from the altitudes of 700 meters to the sea level (Figure 2.24.). The Akyaka village also was built on this slope debris unit which is composed of mainly rock pieces and red soil layer on top.



**Figure 2.24. Sakar mount limestone unit and slope debris on foothills.**



**Figure 2.25. A local slope debris unit in a valley.**

According to field trip observations, slope debris mass units seem very loose and inversely very compacted in some places. It is thought that this unit is also plays a role on the springs which probably supply sub-surface interflow and baseflow. There are some observed spring points (springs numbered: 26 and 33) in the study area which have very low electrical conductivities.

The second geological unit is conglomerate and carbonated clastics which can be observed in light blue colored units in the local hydrogeology map (Figure 2.23.). This unit can be examined near the springs area and it overlies limestone units.



**Figure 2.26. The conglomerate unit near springs area.**

This unit's color changes from red to cream white according to their composition ratio of pebbles and cementation matrix. In some places, sandstone layers underlie horizontally this unit (Figure 2.27.).

**Figure 2.27. An outcrop surface near Kuyucak village.**



**Figure 2.28. Kuyucak high plain village micro-basin.**

The outcrop (Figure 2.27.) is visible in the north-west part of study area where a big block of listric fault block slid rotationally. Due to this geological structure and inclination, a small surface drainage area near Kuyucak was added to the Ula sub-basin and its watershed (Figure 2.28.). Moreover the existence of a vertical fault (Figure 2.29.) cutting limestone units starting from Çamköy to Kuyucak is a posibble

good path for karstic groudwater flow. Thus, the area which surrounds Kuyucak and Ula may recharge the springs through a fault plane from the valley in the north of Akyaka.



**Figure 2.29. The vertical fault plane near Kuyucak village.**

Limestone unit which is coloured in green in the hydrogeological map, mainly covers the area in north-east part, seems weathered and karstified because of some visible void and cavities. It has crushed layers with numerous discontinuities and small block faults. This unit can be observed on the road-cuts near Akyaka. Google Earth also supplys good images of this unit in its ground level view (Figure 2.30.).



**Figure 2.30. The Google Earth image of the limestone unit.**

Final unit , the Alluvium unit, is visible near main spring outlet. In fact, slope debris and Alluvium meet at that point.



**Figure 2.31. The main spring in the study area.**

The red soil layer is visible over the alluvium unit, but near the main spring crushed rock debris was located as it seen in the picture (Figure 2.31.).

## 2.6. Azmak Stream And Springs

The main study was conducted on Akyaka springs which discharges directly into the flow channel of the Azmak Stream. All measurements were taken from these springs.

The Azmak Stream which was also known as 'Kadın Azmağı' is about 1.8 km long and 35 meters wide maximum on some locations (Figure 2.32.). Since this river system is a protected area, there are some sightseeing boats on the river for tourists (Figure 2.33.). Especially in the summer, this place is really crowded with full of people. It has a clear turquoise color water. According to studies the flow rate of this stream is 11.18 $m^3$/s (Anonymous, DSI) and 10.8 $m^3$/s (Açıkel, 2012).

**Figure 2.32. The Google Earth view of Azmak stream.**



**Figure 2.33. A view from the flow channel of Azmak stream.**

On the north side of the flow channel of Azmak stream springs are located (Figure 2.34.)

31

**Figure 2.34. Measurement locations and numbers.**

In the east, first spring 1, the main spring, discharges in a natural pool zone in the Alluvium unit slope debris contact.
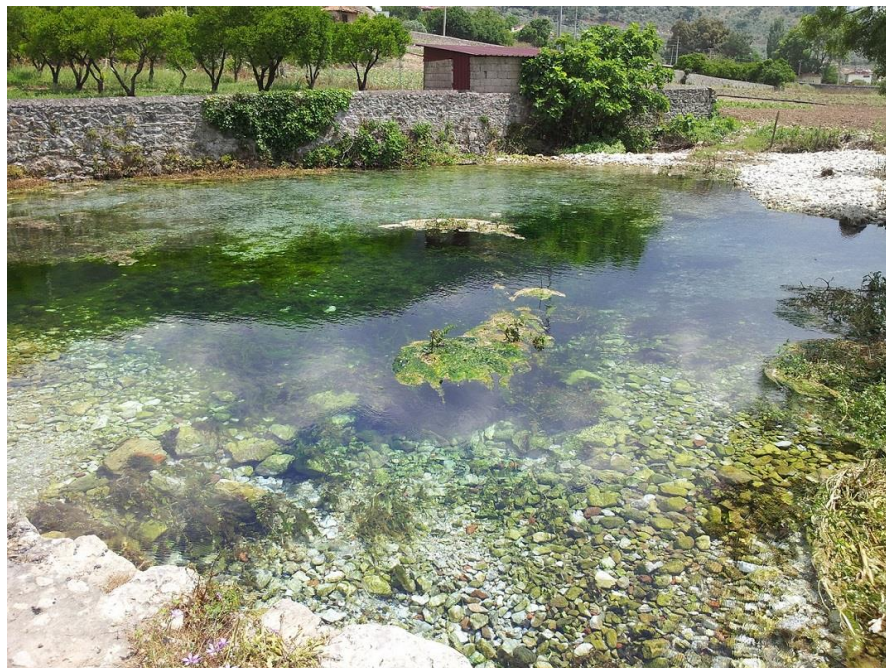


**Figure 2.35. The main spring 1.**

Starting from this (spring 1) spring, measurement locations were given in numbers except number 8 (stream channel), number 48 (stream channel) and number 49

(Sea).(See Figure 2.34.) Other 46 spring points were located from east to west following one by another. On some locations springs are very close to each other about 1-2 meter or in lesser distance. For example in the spring zones of numbered with 3-30 and 38-42.

**Table 2.2. Measurement location numbers and (UTM) coordinates.**

| A | B | C | D | E | F |
|---|---|---|---|---|---|
| 1 | 619355.00 m E | 4101624.00 m N | 26 | 618970.00 m E | 4101855.00 m N |
| 2 | 619331.00 m E | 4101647.00 m N | 27 | 618960.00 m E | 4101859.00 m N |
| 3 | 619209.00 m E | 4101771.00 m N | 28 | 618953.00 m E | 4101860.00 m N |
| 4 | 619173.00 m E | 4101772.00 m N | 29 | 618949.00 m E | 4101858.00 m N |
| 5 | 619159.00 m E | 4101790.00 m N | 30 | 618947.00 m E | 4101852.00 m N |
| 6 | 619144.00 m E | 4101796.00 m N | 31 | 618927.00 m E | 4101856.00 m N |
| 7 | 619130.00 m E | 4101797.00 m N | 32 | 618902.00 m E | 4101873.00 m N |
| 8 | 619117.00 m E | 4101801.00 m N | 33 | 618872.00 m E | 4101911.00 m N |
| 9 | 619106.00 m E | 4101805.00 m N | 34 | 618876.00 m E | 4101905.00 m N |
| 10 | 619098.00 m E | 4101807.00 m N | 35 | 618824.00 m E | 4101918.00 m N |
| 11 | 619090.00 m E | 4101811.00 m N | 36 | 618765.00 m E | 4101921.00 m N |
| 12 | 619085.00 m E | 4101815.00 m N | 37 | 618741.00 m E | 4101922.00 m N |
| 13 | 619079.00 m E | 4101816.00 m N | 38 | 618726.00 m E | 4101926.00 m N |
| 14 | 619069.00 m E | 4101817.00 m N | 39 | 618718.00 m E | 4101927.00 m N |
| 15 | 619064.00 m E | 4101818.00 m N | 40 | 618713.00 m E | 4101927.00 m N |
| 16 | 619053.00 m E | 4101822.00 m N | 41 | 618707.00 m E | 4101928.00 m N |
| 17 | 619046.00 m E | 4101825.00 m N | 42 | 618701.00 m E | 4101928.00 m N |
| 18 | 619038.00 m E | 4101829.00 m N | 43 | 618553.00 m E | 4101904.00 m N |
| 19 | 619031.00 m E | 4101832.00 m N | 44 | 618398.00 m E | 4101752.00 m N |
| 20 | 619024.00 m E | 4101834.00 m N | 45 | 618378.00 m E | 4101737.00 m N |
| 21 | 619019.00 m E | 4101837.00 m N | 46 | 618230.00 m E | 4101617.00 m N |
| 22 | 619013.00 m E | 4101839.00 m N | 47 | 618174.00 m E | 4101562.00 m N |
| 23 | 619007.00 m E | 4101840.00 m N | 48 | 618062.00 m E | 4101289.00 m N |
| 24 | 619000.00 m E | 4101842.00 m N | 49 | 617733.00 m E | 4101240.00 m N |
| 25 | 618982.00 m E | 4101850.00 m N | | | |
| Location Number : Columns A and D , UTM Coordinates: Column B-C for A , Column E-F for D | | | | | |

**Figure 2.36. Spring discharge point 13.**



**Figure 2.37. Spring discharge point 12.**

**Figure 2.38. Spring discharge point 18.**

There were also temporary springs which stayed 2 weeks or 1 month and then disappeared, some did suddenly and some did gradually.



**Figure 2.39. Unrecorded temporary springs.**

# 3. MATERIAL AND METHOD

## 3.1. Material

### 3.1.1. Measurement devices for field study

The devices which were used to acquire data in the field were Horiba U-52 multi-sampling water quality measurement device and Extech EC-400 Electrical Conductivity measurement device.

According to Horiba U-52 multi-sampling measurement device manual, it measures temperature with 0.01 ˚C resolution in -10 to +55 ˚C temperature range by using a JIS Class B (0.3 + 0.005 [t] ) Platinum temperature sensor.

Electrical Conductivity is measured with (0.001) - (0.01) - (0.1) precision in order (0-0.999 mS/cm) - (1 – 9.99 mS/cm) – (10- 99.9 mS/cm) ranges of electrical conductivity values by using a four AC electrode. It gives specific electrical conductance values automatically corrected to 25 ˚C.

For pH values it uses glass electrode and gives results in 0 to 14 pH unit range with 0.01 resolution and 0.1 pH unit precision. The pH 7 ultra-pure solution used regularly for checking measurement accuracy and stability at 25 ˚C.

TDS values are a function conversion of EC values in g/L. Measurement range is 0-100 g/L with 0.1 % resolution of full scale and 5 g/L precision.

Sea water specific gravity values can be measured in a range of 0 to 50 σt with 0.1 σt resolution(http://www.horiba.com/fileadmin/uploads/ProcessEnvironmental/Documents/U-50_Manual_revised_0409.pdf, Anonymous, 2015).

The Extech EC-400 Electrical Conductivity measurement device is capable of measuring electrical conductivity from 0 to 19.99 mS/cm in three stages with 2% accuracy of full scale for each measurement stage (http://www.extech.com/instruments/resources/manuals/ec400_um.pdf, Anonymous, 2015).

Laboratory thermometers were used for calibration and field check before measurement.

### 3.1.2. Materials for device maintenance and laboratory study

Field data measurement devices initially calibrated with calibration solutions which were given with devices. Each of them checked and readjusted in every two weeks periodically. General two months maintenances were also applied to devices as mentioned in their manual papers which came with products (For manual paper link See Page 36).

The materials which were used in calibration process were pH 4-7 solutions, 100 - 500 µS/cm and 10 mS/cm KCI reference solutions which were prepared in a chemistry laboratory of Muğla Sıtkı Koçman university.

Temperature sensor calibration and adjustments were done with laboratory grade thermometers. Two laboratory grade thermometer. One 0-100 ˚C. Another 0-65 ˚C. With 0.5 and 0.1 ˚C precision.

For water analysis of major elements, 500 ml HDPE bottles were used. 0.45µm filters and 65% $HNO_3$ were used to conserve the water samples in good condition.

### 3.2. Research Methodology

The main idea when selecting this methods for this thesis study was to reveal the specific and the dominant type of sea water mixing mechanism, which is playing the main role on Akyaka karst springs. In preliminary studies, Açıkel (2012) mentioned about possible sea water mixing mechanisms based on the montly taken temperature and specific EC data of springs.

To understand the mixing zones precisely and to define the dominant mixing type, springs were observed every week periodically in a 7 months time duration, where flow rate measurements are hard and inapplicable. Each week, temperature and specific electrical conductance (SpC) of springs were measured from 46 spring points. Additionally, it is taken measurements on 3 points of which are from Azmak stream and the Sea. (See Figure 2.34., Table 2.2.).

To define the specific type of sea water mixing by catching temperature, SpC and pH change signals, a new method, inspired from sound wave spectrum analysis in sound

engineering, was applied in this chapter. The first advantage of this matrix method is, it shows the changes visually which occurred in a long time duration on springs. Moreover, it is a good method when data is in large amounts.

To support this visual classification method scientifically, water analysis were also made from selected springs.

**Table 3.1. Field Observation dates.**

| 1.st Week | 03/04/2015 | 14.th Week | 01/07/2015 |
|-----------|------------|------------|------------|
| 2.nd Week | 08/04/2015 | 15.th Week | 08/07/2015 |
| 3.th Week | 15/04/2015 | 16.th Week | 15/07/2015 |
| 4.th Week | 22/04/2015 | 17.th Week | 23/07/2015 |
| 5.th Week | 02/05/2015 | 18.th Week | 29/07/2015 |
| 6.th Week | 08/05/2015 | 19.th Week | 06/08/2015 |
| 7.th Week | 14/05/2015 | 20.th Week | 12/08/2015 |
| 8.th Week | 21/05/2015 | 21.th Week | 19/08/2015 |
| 9.th Week | 27/05/2015 | 22.th Week | 26/08/2015 |
| 10.th Week | 04/06/2015 | 23.th Week | 02/09/2015 |
| 11.th Week | 11/06/2015 | 24.th Week | 08/09/2015 |
| 12.th Week | 17/06/2015 | 25.th Week | 16/09/2015 |
| 13.th Week | 24/06/2015 | Date format | dd/mm/yyyy |



**Figure 3.1. A picture showing the data recording process in the field.**

38

### 3.2.1. Matrix method

*3.2.1.1. Matrix notation*

Matrix is a mathematical way of showing related or non-related numbers in columns and rows by constructing a rectangular shape form (Equation 3.1).

$$\mathbf{Z} = \begin{bmatrix} 1 & 0 & 4 & 0 \\ 1 & 0 & 7 & 1 \\ 1 & 4 & 5 & 3 \\ 1 & 9 & 2 & 3 \end{bmatrix} \tag{3.1}$$

Matrices are named with Capital letters and covered with box brackets in general. In this $\mathbf{Z}$ matrix, the vertical column structure indicated in green colour and the horizontal row structure indicated in blue colour. The value coloured in red on the left upper corner is accepted as ($z_{11}$) which means it is the element of first column and first row. Respectively, due to row and column place orders elements get their location names. The value on the right bottom corner in orange colour is the element of fourth column and fourth row as ($z_{44}$) (Sullivan and Unwin, 2010).

*3.2.1.2. Temperature, specific electrical conductance and pH matrices*

The temperature, SpC and pH data which has been taken weekly from April 2015 to the end of September 2015 was arranged separately to form a matrix structure in an Excel file. Despite 29 weeks of data were taken, 25 weeks of data was used to form a matrix structure because of the continuity of the data between April and September.

39
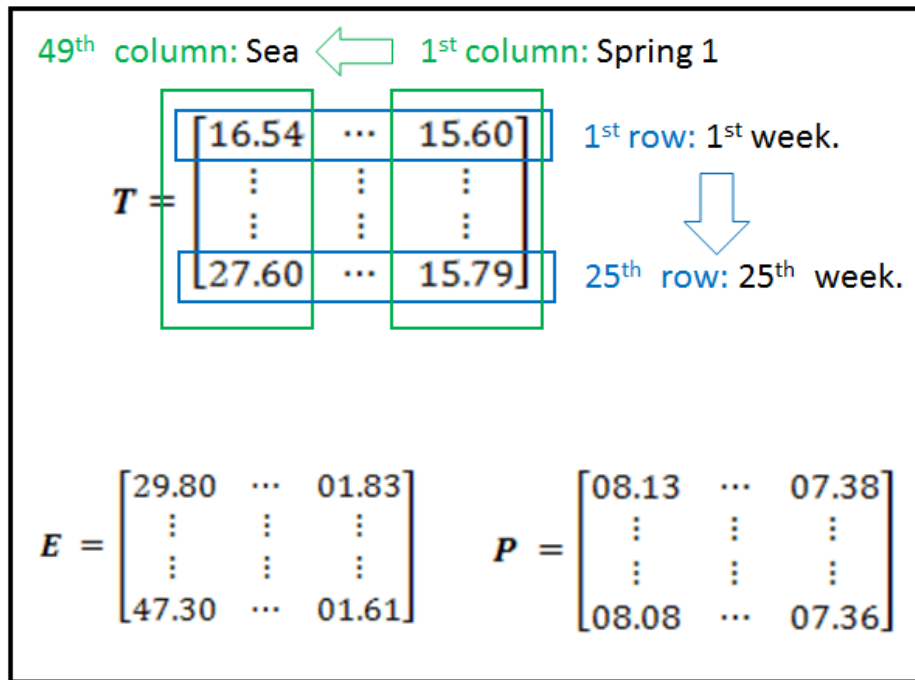
**Figure 3.2. The data structure of matrices.**

The temperature matrix $T$ (3.2), $E$ (3.3) SpC matrix and $P$ (3.4) pH matrix each consist of [26X50] values of data. 25 weeks data fills (Y) axis as rows. Each row represents a week. 49 measurement points aligned in order on (X) axis. Automatically, MatLAB R2013a software arranges the matrices to a [25X49] matrix structure due to cell producing process. $50^{th}$ column and $26^{th}$ row are essential pseudo columns for preventing the automatic cut-off when the program is turning data into cell structures by using "*surf()*" command. Each column represents the change function in temperature, specific electrical conductance and pH units by time. MatLAB automatically constructs faceted cells using matrix data for each element of the related matrices ($z_{yx}$). Further information about data processing algorithms of MatLAB can be obtained from its official web page (www.mathworks.com ).

After $T, E$ and $P$ matrices were prepared in a specific structure (See Figure 3.2.) in Excel worksheets, they were given to the MatLAB programme by its data import feature. In the command line, by using *surf(T)* , *surf(E)* and *surf(P)* commands, the matrices were plotted.

40
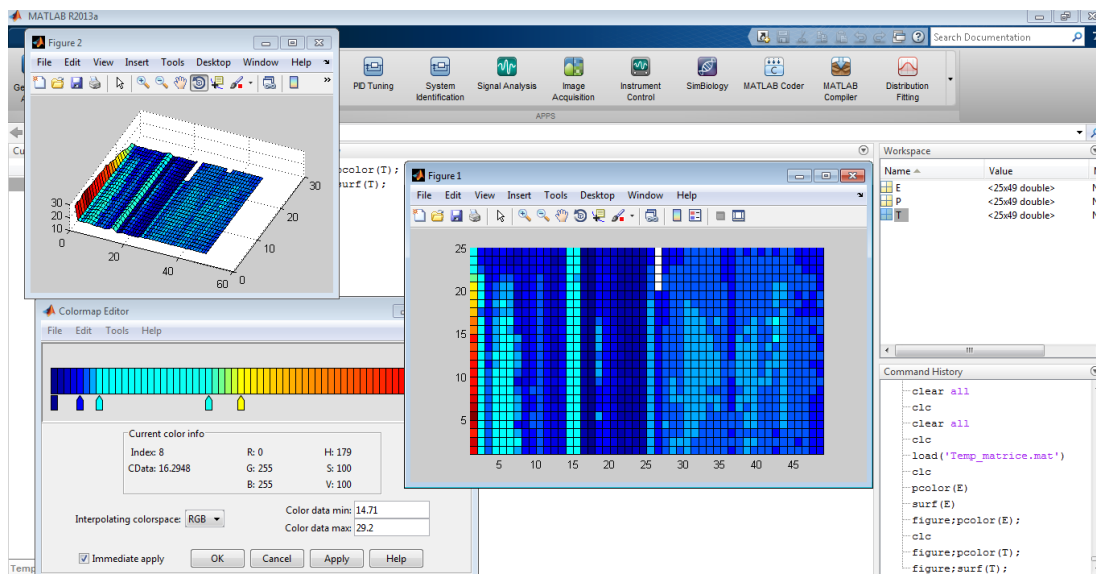
**Figure 3.3. A screenshot from matrix data processing.**

If the 3-D feature is not very important, the "*pcolor()*" 2-D command can be used. Considering the fact that, it is an automatic programme and it will assign the ($z_{yx}$) elements to temperature, SpC and pH values, the final matrix surface images will be linearly interpolated into colour tones. To adjust and see the small changes, the "*colour-map*" feature must be checked and tuned according to real value ranges.

### 3.2.2. Supplementary methods

*3.2.2.1 Water sampling and chemical analysis*

After plotting physico-chemical property matrices, some water samples were taken from selected springs. The sample selection was made according to data analysis and visual distinctive properties of springs which were obtained from matrice graphics.

In the field, each 500 ml HDPE bottle precleaned with pure water and then rinsed with related spring water a few times. Additionally, two samples were taken from each spring and one of them was acidified with %65 $HNO_3$ for ionic protection. The water samples were from Spring 1 (Main spring), Spring 14 (representing the long spring zone), Spring 26, Spring 35 (Highest EC), Spring 40 (Moderate EC and cold springs), Spring 47 (the last spring) and Seawater.

**Figure 3.4. Water sampling materials.**



**Figure 3.5. A picture from water sampling in the field.**

After sampling in the field, water samples were sent to the analysis laboratory.

The Na, K, Ca, Mg, CI, $SO_4$ ion analysis were made by using DIONEX ICS 3000 ion chromatography device.

According to obtained information from the authority of the laboratory:

As soon as samples were gotten, they were refiltered and prepared for analysis.

$CO_3$ and $HCO_3$ ionic analysis were made by applying a titrimetric method to water samples using 0.01 N $H_2SO_4$ solution.

All water samples were diluted 25 times and seawater sample was diluted 500 times before water analysis.

# 4. FINDINGS AND RESULTS

## 4.1. Matrix Method Results

In this section the matrix results which had been plotted by MatLAB were presented, inspected and analysed in respect with field observations and measurements. Each matrix image was plotted three times in the related programme before publishing in this thesis to make sure that no error occurred caused by the computer software. Finally two matrix images were plotted for each physico-chemical property. One of them shows all sampling locations especially including Seawater data (the location number 49). The other matrix image shows springs and Azmak stream flow-channel data (the location number 8 (the starting point) and the number 48 (the end of the flow channel)).

## 4.1.1. The temperature matrix and findings

The consequential images of the matrix method based on Temperature values was given in the following figures (Figure 4.1. and Figure 4.2.)
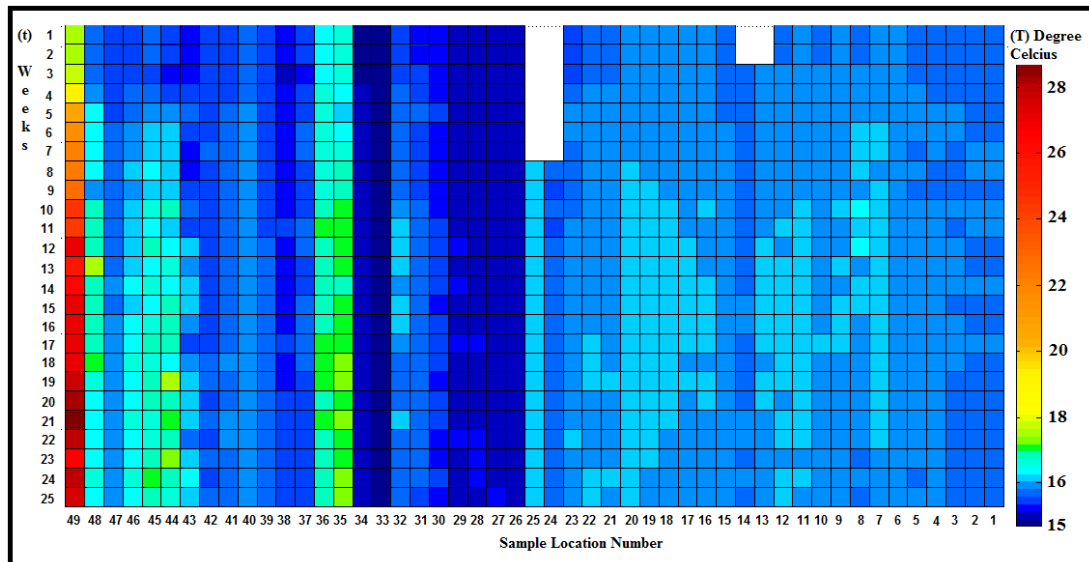


**Figure 4.1. The temperature matrix of all sampling locations.**

44

**Figure 4.2. The more detailed temperature matrix image of springs.**

According to logged data and this temperature matrices plotted in MatLAB, findings were obtained and listed below.

- The sea water started warming in 4.th week of observation and the following week, the 5.th week, the end of the Azmak stream channel and the springs numbered with 7, 8, 20, 44, 45 started warming.

- The seawater draw a linear temperature increase starting from 17.05 ˚C in the first week and 28.00 ˚C maximum in 21.st week of observation.

- In the 8.th week, two new springs (24-25) were born and the remarkable thing was the water temperature of the 25.th spring which was 16.06 ˚C.

- The initial temperature value of the springs located in the range of 2 to 25 was around 15.80 ˚C. They got warmed in the following weeks reaching the temperature values of 16.20 ˚C maximum and a mean value of 16.00˚C. In the last week of observation most of the springs turned back to their initial temperatures or so close values in the range between 15.80 ˚C - 16.10 ˚C.

- The spring 26 was one of the springs which has relatively cold water. With the initial temperature value of 14.96 ˚C it was the second coldest spring. From the spring 26 to spring 30, these springs have a mean temperature value of 15.14 ˚C and the maximum temperature value of 15.30 ˚C.

- The spring 33 was the coldest spring which has temperature values ranging from 14.71 ˚C to 14.85 ˚C.

45

- The spring 35 is the spring which has the highest temperature value. Having the temperature values ranging from 16.27 ˚C to 17.38 ˚C. As it seems in matrix images it showed an increasing trend over time parallel to the seawater temperature change. The spring 34 also did the same behaviour.

- The spring zone consist of numbers 37 to 43 are a group of springs located very close to each other. These spring group has a mean temperature value of 15.63 ˚C, having the initial temperatures starting around 15.40 ˚C to 16.04 ˚C maximum.

- The final group of springs consist from the springs starting from number 44 to number 47. All springs in this group except the spring 47 have small pools that have low level recharge. These springs showed increasing temperature values probably due to the air and soil temperature increase in the summer. However the spring 47 is a big and permanently flowing spring. Having the temperatures starting from 15.53 ˚C to 16.03 ˚C. This spring also showed an increasing temperature trend in a very narrow range.

As a result of increasing temperature in springs (5.th week) in parallel with increasing sea water temperature (4.th week), it can be concluded that the seawater which is mixed with fresh water comes from the shallow zone of Gökova Bay.

### 4.1.2. The specific electrical conductance matrix and findings

The consequential images of the matrix method based on SpC values was given in the following figures (Figure 4.3. and Figure 4.4.).



**Figure 4.3. The specific electrical conductance matrix of all sampling locations.**



**Figure 4.4. The more detailed specific electrical conductance matrix image of springs.**

According to logged data and this specific electrical conductance matrices plotted in MatLAB, findings were obtained and listed below.

- The SpC of the seawater varied between 30.20 mS/cm and 49.50 mS/cm in a seven months time period. Having a mean SpC value of 39.79 mS/cm, it

showed a main increasing trend with some minor local deacreasing and increasing trends starting from April 2015 to the end of September 2015.

- First 2 springs which were almost the same springs, they have consisted SpC values varying between 1.61 mS/cm and 2.02 mS/cm.

- The salinization was clearly noticeable in the 6.th spring with a SpC value of 6 mS/cm. In the 14.th spring it was a little bit diluted with a starting value of 5.90 mS/cm and final 3.37 mS/cm ending value.

- The 25.th spring had SpC values changing from 7.70 mS/cm to 10.30 mS/cm mainly showing an decreasing trend over time.

- In springs 26, 27 and 28 which were located very closely about 1 meter far from each other showed almost same results. These springs have very low SpC values ranging from 1.73, meanly 2.18, rarely to the maximum value of 3.08 mS/cm. All of them showed a decreasing trend.

- For the springs starting from 30 to 42 except the springs 33, a mixing zone is visible againg especially in the 35.th spring which is the spring that had the highest SpC value 18.50 mS/cm. By showing a decreasing trend in SpC, it had its lowest value in the last week of observation the 25.th week.

- The spring group consisting of 37 to 42 had SpC values between minimum 5.32 mS/cm to maximum 13.00 mS/cm and mean value of 8.74 mS/cm. The 40.th spring had the highest SpC value. As it seen in the related figures, they had decreasing values over time.

- The springs 43, 44, 45 which have small pools have the same maximum to minimum manner as other springs.

- The springs 46 and 47 shows different SpC characteristics having the values between 4.68 mS/cm and 6.03 mS/cm, meanly 5.35 mS/cm. The spring 46 showed a bell shape increasing to decreasing behaviour. On the other hand, the spring 47 showed slowly decreasing trend specifically in the last weeks of observation.

As a conclusion almost all of the springs are under control of a specific type of Sea water mixing mechanism, because nearly all of them showed decreasing trend in SpC values.

### 4.1.3. The pH matrix and findings

The consequential images of the matrix method based on pH values was given in the following figures (Figure 4.5. and Figure 4.6.)
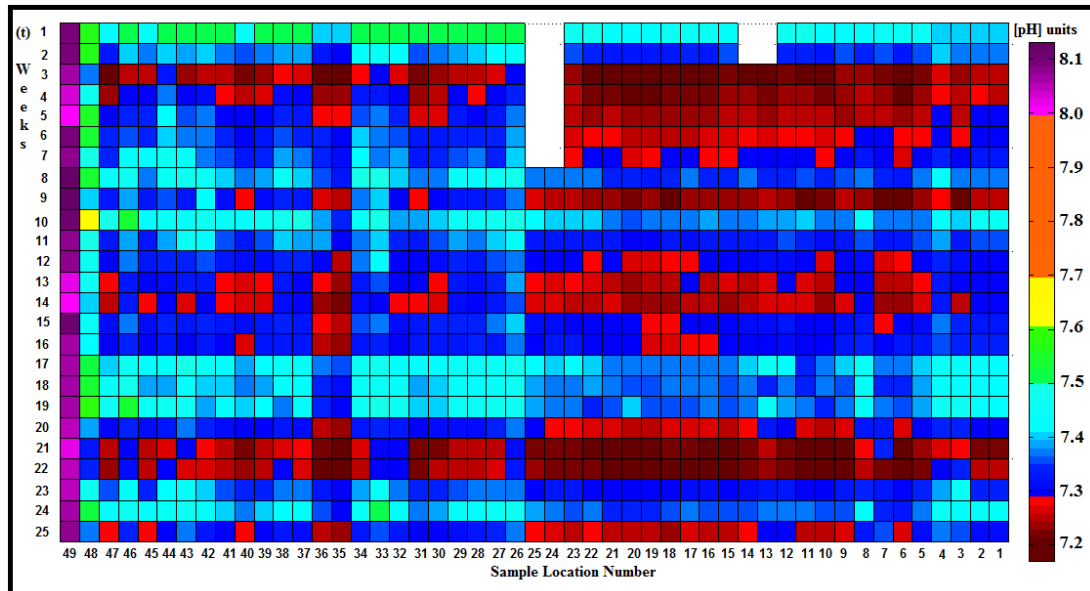


**Figure 4.5. The pH matrix of all sampling locations.**



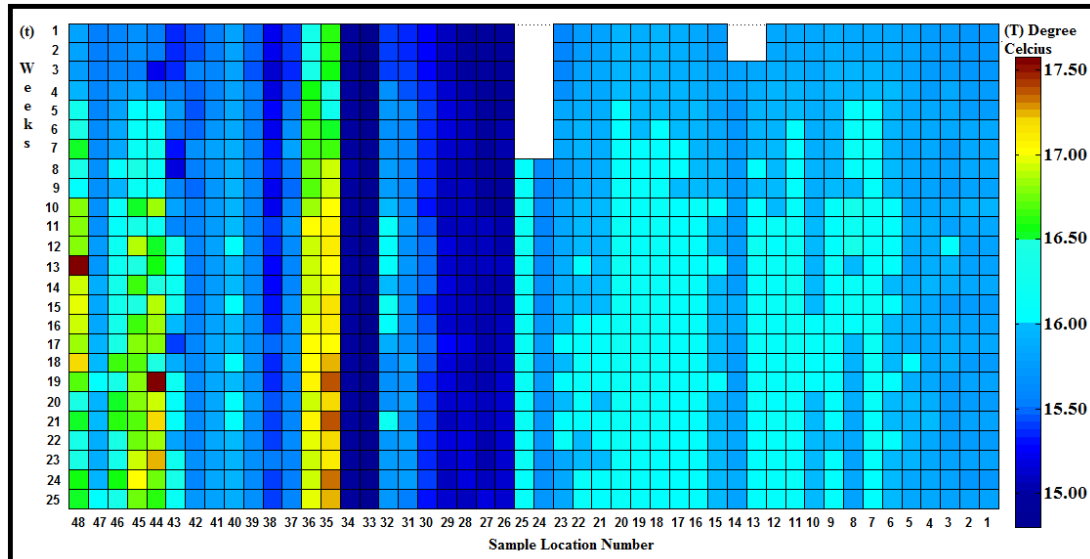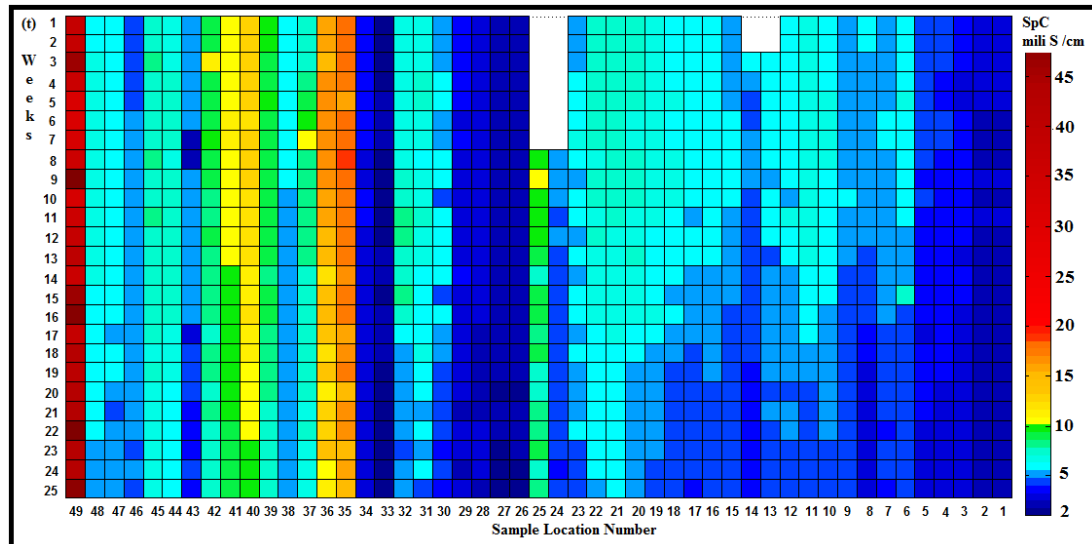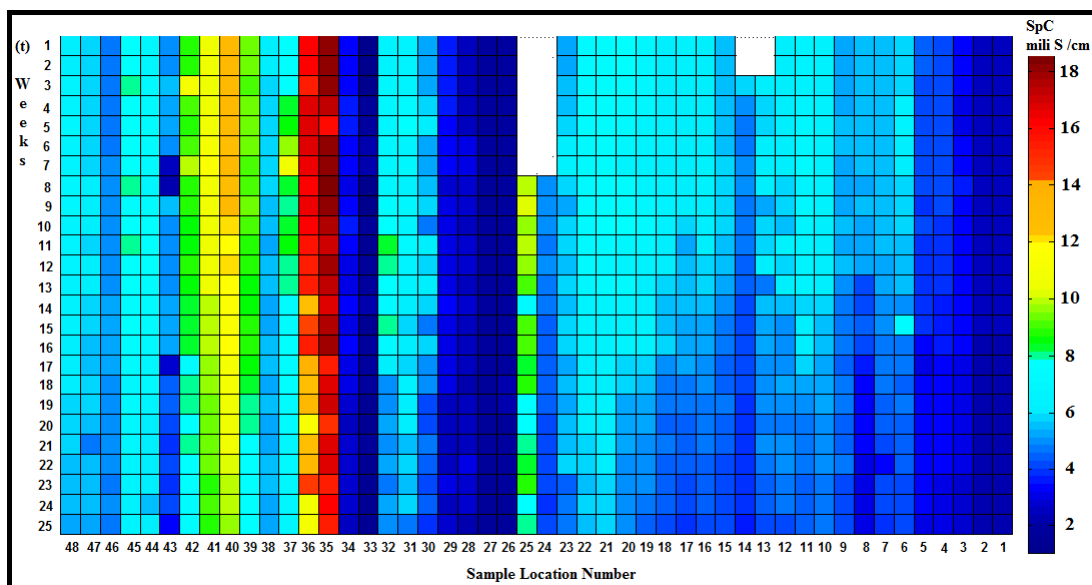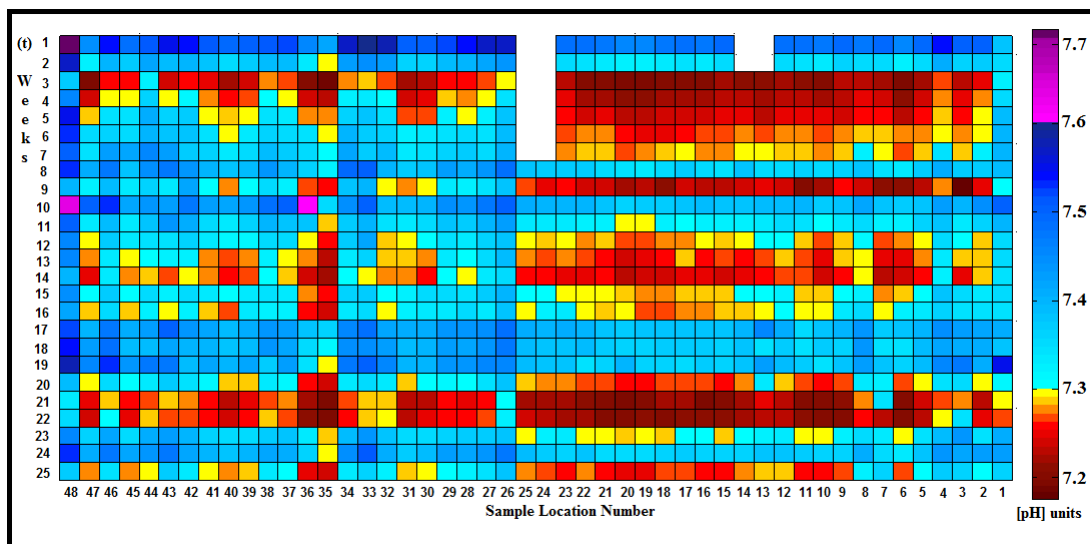**Figure 4.6. The more detailed pH matrix image of springs.**

According to logged data and this pH matrices plotted in MatLAB, findings were obtained and listed below.

- In 3.th week of observation, the first visible change was noticed in pH measurements. While pH values were over 7.30 in 2.nd week, the 3.th week values were around 7.20. The following weeks of that week their pH values gradually raised. This phenomenon repeated 4 times. Two times in a small scale which is only one week, two times in a relatively big scale 4-6 weeks as the first time happened in 3.th week.

- The Sea water (49.th location) pH values started with 8.13 pH units and showed a decreasing trend having fluctuations in some weeks. It had a minimal value of 8.00 pH units.

- The first spring had changing pH values ranging from 7.27 pH units minimum to 7.55 pH units maximum. Lower values recorded 21.th and 22.nd weeks only.

- The springs marked with numbers between 2 and 25 except the number 8.th which is stream channel control point , this spring group almost showed the same pH behaviour during all observation weeks. The pH value varied between 7.19 pH units minimum and 7.51 pH units maximum, having the mean pH value of 7.32 pH units.

- The spring 26 affected from that phenomenon also. Its pH values fluctuated between 7.31 and 7.51 pH units with an average pH value of 7.41.

- The 33.th spring, which had the lowest temperature and SpC values, had the highest pH value 7.60 pH units. Its minimum pH value was 7.29 pH units and its average pH value is 7.40 pH units.

- The 35.th spring, which had the highest temperature and SpC values had the lowest pH value 7.18 pH units, having the average pH value of 7.28 pH values. The slow increasing and decreasing effect in pH values, before and after weeks of the lowest pH week, clearly visible in this spring.

- The spring zone 37-42 showed related periodically fluctuation effect. Their average pH value is 7.35. Maximum and minimum value of pH in this group were 7.54 pH units in spring 42 and 7.22 pH units in spring 40. Especially, 40.th spring which is in the middle of the spring group is sensitive to small changes.

- Springs 46 and 47, especially the spring 47 is a spring which discharges with a considerable high flow rate during a year time. In its matrix column of data,

as it seen in the image, it got affected from the fluctuation effect. It has a maximum value of 7.50 pH units and minimum value of 7.19 pH units, average value of 7.33 pH units in a time period of seven months observation.

- The 48. th column show the historical change of pH at the end of Azmak stream channel. It presented a decreasing manner with fluctuated values between in a range of 7.37 and 7.77 pH units.

As a conclusion for this section, a fluctuation movement in pH values are detected from the pH matrix image of the springs.

The decrease in pH values probably caused by sea level rise and sea water intrusion. Thus this mixing process is visible as pH fluctuations on springs. This pH drop was explained in discussion section by using the information which was obtained from Ford and Williams, (2013) "*Karst hydrogeology and geomorphology*" book.

## 4.2. Chemical Analysis Results

The springs which represent different zones and have specific values were chosen for chemical analysis. After results were received, the error analysis of chemical analysis results was made to have an idea about the analysis quality of water samples.

The formula (3.5) (Ford and Williams, 2013) was used for percentage error calculation:

$$\text{IBE (\%) error} = \left| \frac{\Sigma(\text{Cations} - \text{Anions})}{\Sigma(\text{Cations} + \text{Anions})} \right| \times 100 \tag{3.5}$$

This formula gives an idea about the quality of the analysis. The percentages below 5% are accepted as good results. However, for some water samples which contain other ions can cause high error rates.

The ion concentrations were converted to meq/L in units and error ratios were calculated.

**Table 4.1. The error (%) values of water analysis results.**

| Sample | % Error |
|---|---|
| Spring 1 | 7.34 |
| Spring 14 | 16.06 |
| Spring 26 | 8.58 |
| Spring 35 | 19.97 |
| Spring 40 | 19.43 |
| Spring 47 | 17.00 |
| Seawater | 0.52 |

Based on this results, a high error rate is noticeable and over %5 error is not acceptable as good analysis results. However, limited personal financial conditions were not enough to reanalyse the samples. Even though having this rates, at least the water types of the selected springs could be predictable and it was done by drawing the "Piper" and "Schöeller" diagrams.

### 4.2.1. The Piper diagram of selected springs
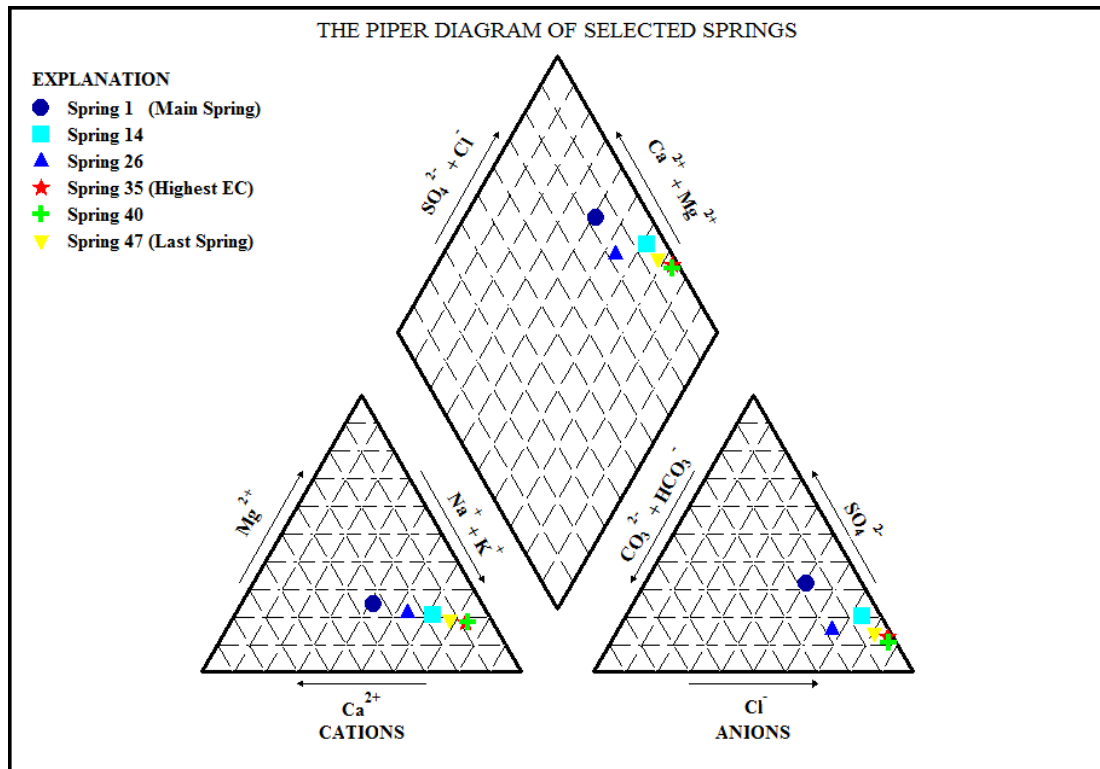


**Figure 4.7. The Piper diagram of selected springs.**

Piper water diagram was plotted by using the free Software, named "GW_chart", which was provided from the web page of USGS (http://water.usgs.gov/nrp/gwsoftware/GW_Chart/GW_Chart.html, Anonymous, 2015).

According to chemical analysis results the dominant ion classification was made for each spring.

The spring 1   : $Na>Ca>Mg>K$ and $CI>SO_4>HCO_3$

The spring 14 : $Na>Ca>Mg>K$ and $CI>SO_4>HCO_3$

The spring 26 : Na>Ca>Mg>K and CI>***HCO_3***>SO_4

The spring 35 : **Na**>**Mg**>**Ca**>**K** and **CI**>**SO_4**>**HCO_3**         *

The spring 40 : **Na**>**Mg**>**Ca**>**K** and **CI**>**SO_4**>**HCO_3**         *

The spring 47 : $Na>Ca>Mg>K$ and $CI>SO_4>HCO_3$

The Seawater: **Na**>**Mg**>**Ca**>**K** and **CI**>**SO_4**>**HCO_3**>CO_3   *

53

Seawater and other high SpC mix water springs referenced with "*" mark to indicate the seawater mix. Also, as it seen in the diagram springs were populated at Na and CI ion corners. It shows these ions are dominant ions in the water.

The spring samples 35 and 40 had high mixing ratio with seawater. Springs 1, 14, 47 showed the same mixing mechanism in different concentrations changing in respect to distance from the sea. The Calcium and Bicarbonate concentrations indicated these waters were oversaturated probably because of mixing with seawater which have high partial carbon dioxide levels.

The spring 26, low SpC and cold water spring, showed some effects of seawater mixing by still preserving its real origin. Its groundwater path is probably shallower than others.

### 4.2.2. The Schöller diagram of selected springs

The other type of water classification diagram "Schöller diagram" was made by using Microsoft Excel Programme.
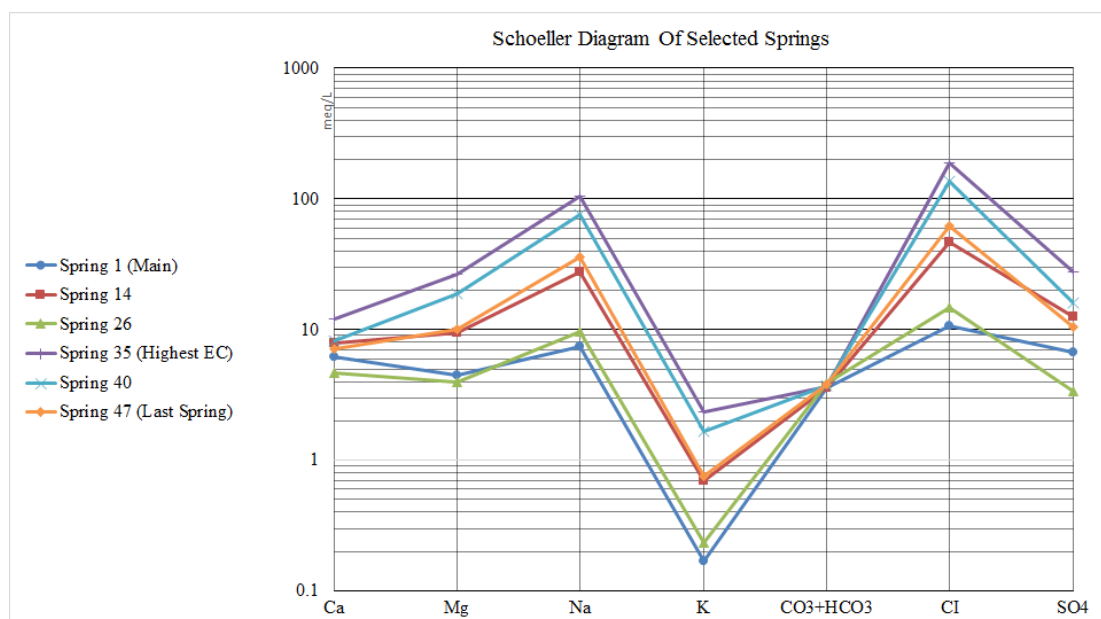


**Figure 4.8. The Schöller diagram of selected springs.**

According to Schöller diagram showing selected springs, it is clear that the dominant cation and anion were Na and CI for all springs. The interesting thing was that the $HCO_3$ concentrations of all springs were very close. This diagram is useful for quick

evaluation of water samples and this is the main reason for adding this extra water classification diagram in this chapter.

### 4.2.3 Saturation indices

Saturation indice values of dolomite and calcite for selected springs was calculated by using the saturation indice formula of each mineral.

$$SIc = log[Ca] + log[HCO3] + pH - pK2 + pKc \qquad (4.10)$$

$$SId = log[Ca] + log[Mg] + 2\,log[HCO3] + 2pH - 2pK2 + pKd \qquad (4.11)$$

The saturation indices were plotted for each spring and seawater.
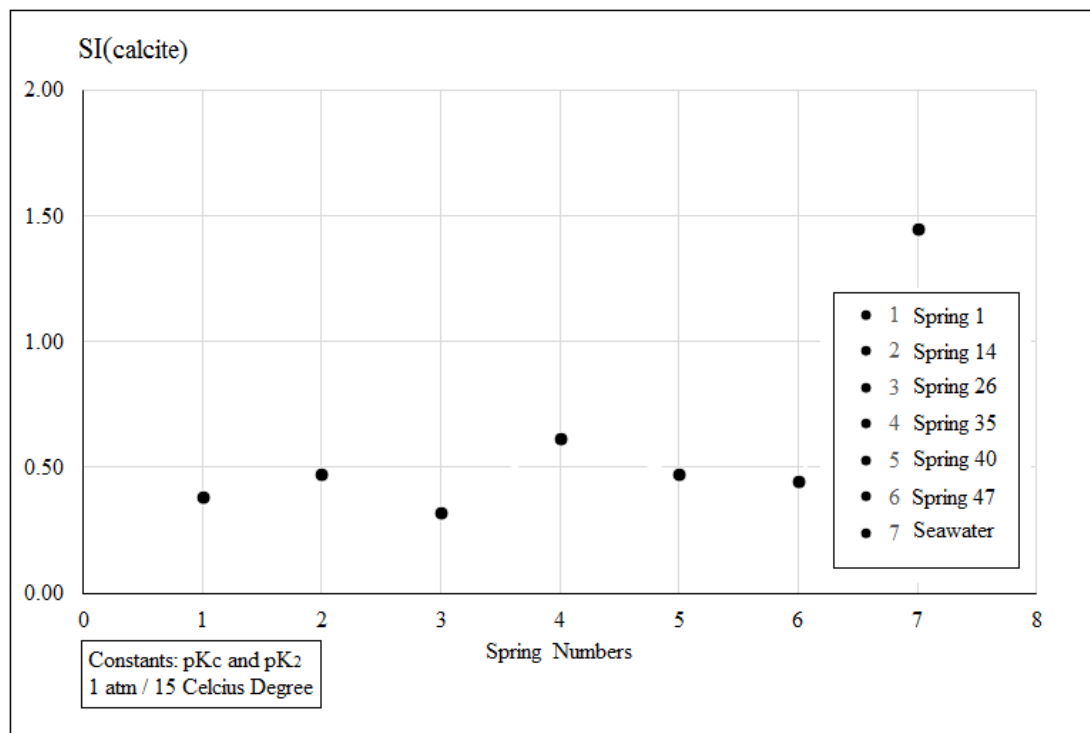


**Figure 4.9. The saturation indices for calcite solubility.**

According to this saturation indice values, the value "0" shows the equilibrium, it can be concluded that all springs were oversaturated to calcite at sea level, 1 atm, 15 ˚C conditions.
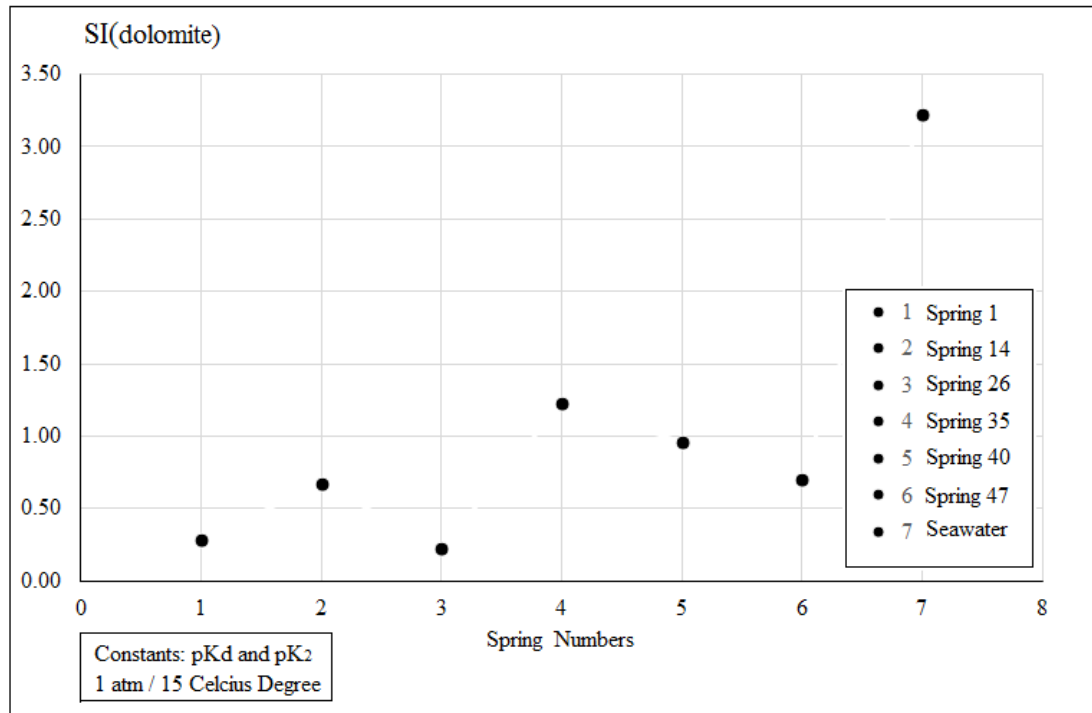


**Figure 4.10. The saturation indices for dolomite solubility.**

For the case of dolomite, it can be concluded that all springs are oversaturated to dolomite at sea level, 1 atm, 15 ˚C conditions.

According to these saturation results, it can be thought that the oversaturation might have been caused by the high partial pressure of carbon dioxide in seawater which drops the pH of mixing water.

All formulas (Equation (4.10) and (4.11) ) and constant values were taken from Ford and Williams (2013).

# 5. CONCLUSION

Depending on the findings and results of the matrix method applied for Akyaka (Gökova) karst springs, after a seven months observation period, it can be concluded that the matrix method gave quick, easy and visible results for engineering judgement to identify some unknown points on the current sea water intrusion mechanism.

According to results, seawater intrusion has visual effects in all matrices at 3.th, 9.th, 14.th, 21.th and 25.th weeks of observation. Especially, in SpC and pH matrices at 3.th and 9.th weeks. The temperature rise in springs also supports SpC and pH matrices.

The SpC values were in a decreasing trend in almost all springs as it clearly seen in the matrices.

The pH values of springs had a decreasing trend in time by having oscillations which was probably caused by seawater intrusion. It is thought that those pH oscillations, especially low pH values indicate the times when the seawater intrusion was high in springs. At those times, the pH of the mixing water is slightly less, about 0.1 pH units than the regular pH range of the spring water.

As a summary, feature anomalies generally were observed in seawater at first and then in the following weeks changes were observed in springs. It can be concluded that the seawater which involves into the mixing comes from the shallow depths of Gökova Bay not from deep seawater.

Having known that the SpC values were in an increasing trend starting from January to March in a year time (Açıkel, 2012). By summing this fact with the findings of this thesis results, it can be thought that the venturi effect might be the predominant agent for seawater intrusion in this area in spring months. However, in summer months, springs were affected from short term seasonal changes and also probably from tidal changes depending on the findings obtained from temperature, specific electrical conductance and pH matrices.

# 6. DISCUSSION

## 6.1. Neighbourhood Basins And Possible Groundwater Recharge

The purpose of adding this section to this thesis study is just to add a contribution to initial studies. There are two basin contact points which may contribute from one to another via subsurface flow system although their surface drainage paths separated by geological factors.
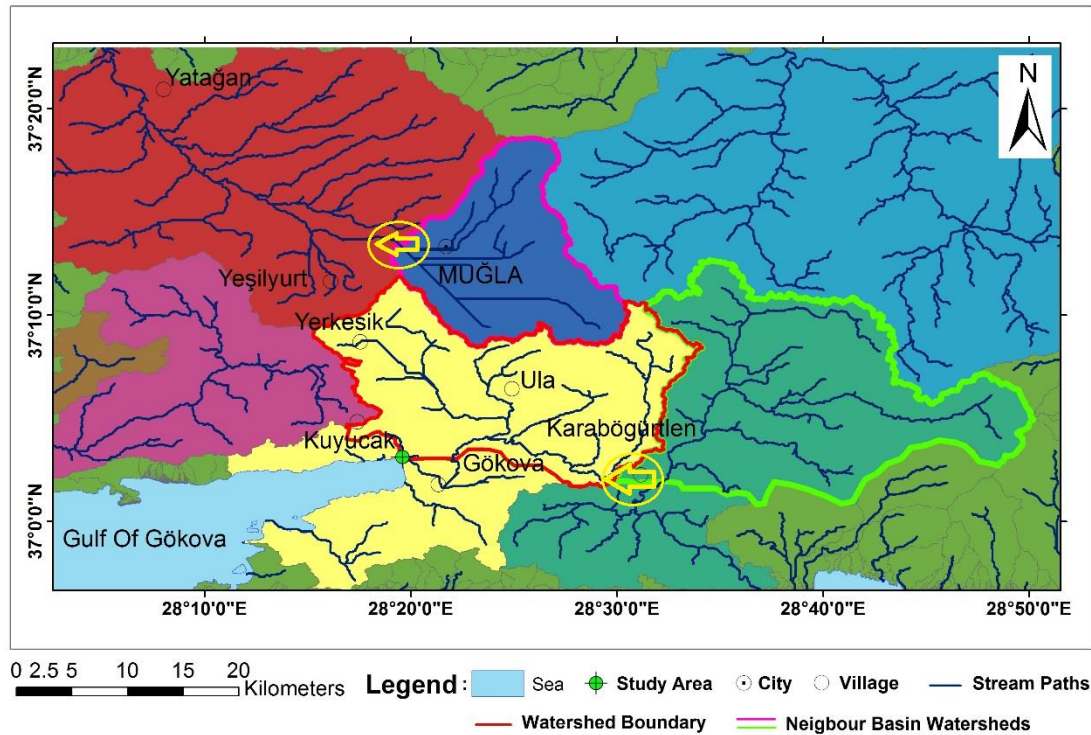


Figure 6.1. The hydrological map which shows neigbour drainage basins.

Despite there is no groundwater tracer experiments except meteoric isotope analysis, it is claimed that the Muğla closed basin (coloured in pink) supports Akyaka karst springs in preliminary studies. Beside this theory, it has been wanted to add a new theoretical view.

Muğla closed basin could supply water for Akyaka karst springs via groundwater system as it lies on Jurassic marbles. However, from a different point of view, It could supply water for yatağan basin via groundwater system since it seems like it had been a part of yatağan basin until it was cut and separeted by a fault system in

the west. The surface drainage pattern and direction can be accepted as an evidence for this theory. Moreover, the groundwater flow might reach to Aydın basin which has active geothermal exploitation sites.

It has been found a neigbour basin (Figure 6.1., coloured in green) which normally feeds Köyceğiz Lake near Karaböğürtlen Village in the east of study area. It is suspected that this neigbour basin could supply water for Ula sub-basin because they are geologically connected with an Alluvium unit which has water wells inside approximately 20 meters deep.



**Figure 6.2. Google Earth image of alluvium unit near Karaböğürtlen village.**



**Figure 6.3. A field picture of the alluvium unit.**

The yellow rectangle and the spot in (Figure 6.2.) shows the location where the (Figure 6.3.) was taken from.

## 6.2. The pH Drop Of Mixing Water Which Contain Sea And Karst Water.

It is known that the solubility of $CaCO_3$ in pure water is about 14 mg/L at 25 ˚C (Ford and Williams 2013). However, this situation changes when $CO_2$ involved into the water system producing $H_2CO_3$, carbonic acid, and so pH of the water declines.

Keeping in mind that $CO_2$ is the most soluble atmospheric gas, which is 64 times more soluble than $N_2$ (Ford and Williams 2013). Additionally, the other point that should be considered is the "Henry`s law" that states the facts about partial pressures of gasses. According to that law, the solubility of $CO_2$ is proportional to its partial pressure in the system. However, solubility of carbon dioxide decreases when its temperature rises. To explain this pH drop in mixing water, it is good to check chemical processes occurred.

$$CO_{2\ (air)} \leftrightarrow CO_{2\ (aq)} \tag{6.1}$$

Atmospheric and soil zone carbon dioxide naturally enters aquatic systems.

$$CO_{2\ (aq)} + H_2O \leftrightarrow H_2CO_{3\ (aq)} \tag{6.2}$$

Carbon dioxide dissolves in water and forms carbonic acid, later on carbonic acid dissociates into hydrogen and bicarbonate ions.

$$H_2CO_{3\ (aq)} \leftrightarrow H^+ + \boldsymbol{HCO_3} \tag{6.3}$$

$$\boldsymbol{HCO_3} \leftrightarrow H^+ + CO_3 \tag{6.4}$$

In closed systems, meaning that all $CO_2$ is consumed and the bicarbonate reaction reached to equilibrium where pH < 8.3 and the $HCO_3$ ion is predominant. The reaction doesn't work to $CO_3$ direction. The $CO_3$ concentrations are usually

negligible. It (Equation 6.3.) starts to increase bicarbonate concentration until all carbonic acid is consumed. When calcite mineral is available in the system three reactions below take place in water and calcite surface.

$$CaCO_3 + \mathbf{H^+} \leftrightarrow Ca + HCO_3 \qquad\qquad (6.5)$$

$$CaCO_3 + \mathbf{H_2CO_3} \leftrightarrow Ca + 2\ HCO_3 \qquad\qquad (6.6)$$

$$CaCO_3 + H_2O \leftrightarrow Ca + HCO_3 + \mathbf{OH^-} \qquad\qquad (6.7)$$

The reaction (6.5) uses $\mathbf{H^+}$ concentration comes from carbon dioxide, in the reaction (6.6) the carbonic acid is consumed and in the last reaction (6.7) calcite dissolves in water. After a time and when all reactants consumed the system gets saturated.

As a sum of reactions, mostly this equation is given.

$$CaCO_3 + CO_2 + H_2O \leftrightarrow Ca + 2\ HCO_3 \qquad\qquad (6.8)$$

The mechanism which drops pH can be explained by considering the changes occurred in the system. When sea water mixes with carbonated water, the partial pressure of carbon dioxide rises from ( closed system theoretical value) 0.036% to **0.038%** ( at standard atmosphere, at sea level, at 25 ˚C) (Ford and Williams 2013). This means that the system gets extra carbon dioxide and so extra carbonic acid as well. The replenishment of $CO_2$ has been thought as the first cause of pH drop.

Secondly, the temperature rise in sea water is important. Because the temperature rise in mixing water decreases the calcite solubility. After 4.th week of observation to the end of September 2015, the mean sea water temperature is 25.75 ˚C due to temperature data. It is visible in the temperature matrix. When the sea water at 25 ˚C meets with saturated karst water at around 15 ˚C ( the annual mean temperature: 15.06 ˚C) it gets warmed reaching to intermediate temperatures around 17 ˚C with a

theoretical mixing ratio of 5:1 ( an example situation for spring 35, its mean temperature is 17.03 ˚C).

The temperature rise in mixing water precipitates $CaCO_3$. This starts to consume calcium and bicarbonate ions and reverses all carbonate dissolution mechanisms (Equation 6.4 to 6.1) back in direction of reactants.

Increasing salinity in a solution, increases the ionic strength of the related solution due to increasing concentrations of different ions. The increasing ionic strength of a calcite solution increases $CaCO_3$ solubility. This prevents pH drop, however high ionic strength may block the $OH^-$ ion activity in the solution more than Hydrogen ion. Thus, temperature change and partial pressure change of $CO_2$ in the mixing water control the pH of the mixing solution.



**Figure 6.4. The bubbling around spring 40.**

The bubbling (degassing) observed around the springs 25, 35, 40 which has high SpC, especially the spring 40 and spring 25. Chemical analysis results were also supported that these springs were a mixture of seawater and karst water having high amount of Na, CI, Mg, $HCO_3$ concentrations.

## 6.3. Human Effects

The human effect on springs can be seen in the spring zone starting from spring 3 to spring 25. The first human effect which may affect that spring zone is the old castle which is located right behind that zone. This castle has some tunnels beneath its destroyed body.



**Figure 6.5. The old castle area behind the springs.**
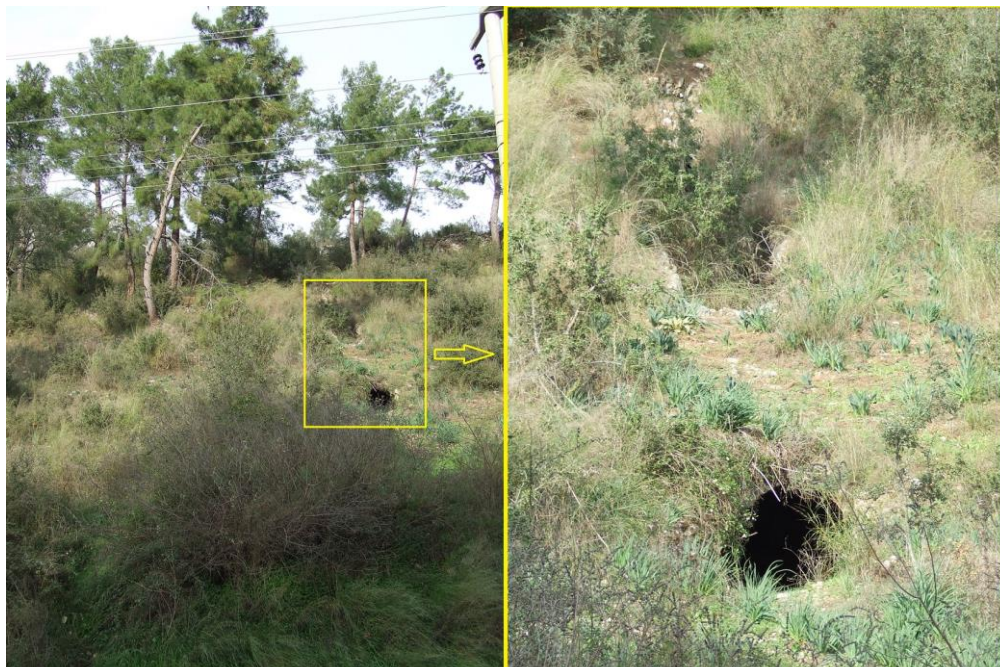


**Figure 6.6. The tunnels beneath the old castle.**

This tunnels also might affect the mixing mechanism of springs which are located in this zone.

The other human effect is the road which was constructed on springs by probably municipality of Ula. To construct the road on Azmak river they placed very big rocks and made a concrete road with an iron skeleton inside. It is observable when you look inside the springs carefully. This structure camouflage the vertical discharge and shows the springs as they are discharging horizontally from the side of the Azmak stream.



**Figure 6.7. The man made road on springs.**

Despite most of the springs seem like they are coming from the north side of the stream, it is observed that some springs comes upward direction just beneath the man made concrete road which changes water movement from vertical to horizontal in some places. Also, in the Azmak stream channel from bottom of the channel to the surface, some springs discharge vertically by giving gas bubbles. This noteworthy phenomenon was observed especially near the springs 40 and 25. Beside, vertically discarging springs in the stream channel were detected by increasing electrical conductivity at some locations.

# REFERENCES

Açıkel, Ş. (2012) *Gökova-Azmak (Muğla) karst kaynaklarında akım ve tuzlu su karışımı dinamiğinin kavramsal modellenmesi,* Doktora Tezi, Hacettepe Üniversitesi, Ankara, 140s.

Anderson, M. P. (2005) Heat as a ground water tracer, *Groundwater*, *43* (6): 951-968.

Baena, C. L., Andreo, B., Mudry, J., and Cantos, F. C. (2009) Groundwater temperature and electrical conductivity as tools to characterize flow patterns in carbonate aquifers: the Sierra de las Nieves karst aquifer, southern Spain, *Hydrogeology Journal*, *17* (4): 843-853.

Bayarı, S., Kazancı, N., Koyuncu, H., Çağlar, S. S., and Gökçe, D. (1995) Determination of the origin of the waters of Köyceğiz Lake, Turkey, *J Hydrology*, 166: 171-191.

Campbell, C. W., El Latif, A., and Foster, J. W. (1996) Application of thermography to karst hydrology, *Journal of Cave and Karst Studies*, *58* (3): 163-167.

Collins, A.S., and Robertson, A.H.F. (1997) Lycian melange, southwestern Turkey: an emplaced Late Cretaceous accretionary complex, Geology, 25: 255– 258.

Collins, A.S., and Robertson, A.H.F. (1998) Processes of Late Cretaceous to Late Miocene episodic thrust-sheet translation in the Lycian Taurides, SW Turkey, J Geol Soc, 155: 759– 772.

Collins, A.S., and Robertson, A.H.F. (1999) Evolution of the Lycian Allochthon, western Turkey, as a north-facing Late Palaeozoic to Mesozoic rift and passive continental margin, Geol J, 34: 107– 138.

Custodio, E., Pascual, J.M. and Bosch, X. (1986) Sea Water Intrusion In Coastal Carbonate Formations In Catalonia, Spain, *Proceedings 9th Salt Water Intrusion Meeting,* 147-164.

Çağlar, I., and Duvarcı, E. (2001) Geoelectric structure of inland area of the Gökova rift, southwest Anatolia and its tectonic implications, *Journal of Geodynamics*, 31: 33-48.

Duriez, A., Marlin, C., Dotsika, E., Massault, M., Noret, A., and Morel, J. L. (2008) Geochemical evidence of seawater intrusion into a coastal geothermal field of central Greece: example of the Thermopylae system, *Environmental geology*, *54* (3): 551-564.

Dürr, S. (1975) *Über Alter und geotektonische Stellung des Menderes-Kristallins, SW Anatolien und seine Aequivalente in der Mittleren Aegaeis*, Thesis, Marburg, Lahn, West Germany.

Dürr, S., Alther, R., Keller, J., Okrusch, M., and Seidel, E. (1978) The median Aegean crystalline belt: stratigraphy, structure, metamorphism and magmatism, In: Closs, H., Roeder, D.R., Schmidt, K. (Eds.), Alps, Apennines, Hellenides, Schweizerbart, Stuttgart, 455– 477.

Ertürk, M., and Atasoy, E. (2010) Kültürel Coğrafya Bakımından Muğla ve Çevre Polyelerde Yaylacılık, *Turkish Studies*, 5: 1264-1296.

Ford, D., and Williams, P. D. (2013) *Karst hydrogeology and geomorphology*, John Wiley & Sons, 576p.

Graciansky, P.C. (1968) Stratigraphie des unites superposees dans le Taurus Lycien et place dans 1'arc Dinaro-Taurique, *MTA Bull*, 71: 42 - 62.

Graciansky, P.C. (1972) *Recherches geologiques dans le Taurus Lycien*, Thesis, University Paris-Sud, France.

Gutnic, M., Monod, O., Poisson, A. and Dumont, J.F. (1979) Geologie des Taurides Occidental, *Mem de la Soc Geol de France*, l37.

Gürer, Ö. F., and Yılmaz, Y. (2002) Geology Of The Ören And Surrounding Areas, Sw Anatolia, *Turkish Journal Of Earth Sciences*, *11* (1): 1-13.

Jensen, M. E., Burman, R. D., and Allen, R. G. (1990) *Evapotranspiration and irrigation water requirements*, ASCE, 360p.

Ketin, İ. (1983) *Türkiye Jeolojisine Genel Bir Bakış,* İstanbul Teknik Üniversitesi Vakfı, İstanbul, 597s.

Konak, N. and Şenel, M. (2002) *Türkiye jeoloji haritası, Denizli paftası 1: 500 000*, Maden Tetkik ve Arama Genel Müdürlüğü, Ankara.

Koralay, O. E., Candan, O., Akal, C., Dora, O. Ö., Chen, F., Satır, M., and Oberhänslı, R. (2011) Menderes Masifi'ndeki Pan-Afrikan Ve Triyas Yaşlı Metagranitoyidlerin Jeolojisi Ve Jeokronolojisi, Batı Anadolu, Türkiye, *MTA Dergisi*, 142: 69-121.

Kresic, N., and Stevanovic, Z. (Eds.). (2009) *Groundwater hydrology of springs: engineering, theory, management and sustainability*, Butterworth-Heinemann, 592p.

Kurttaş, T. (1997) *Gökova (Muğla) Karst Kaynaklarının Çevresel İzotop İncelemesi,* Doktora Tezi, Hacettepe Üniversitesi, Ankara, 220s.

Kurttas, T. and Bayari, S. (1999) Salinization effect of Seawater Fluctuations on coastal springs; Example of Gökova Karstic Springs, *Bulletin of Earth Sciences Application and Research Center of Hacettepe University*, 21: 185-200.

Long, A. J., and Gilcrease, P. C. (2009) A one-dimensional heat-transport model for conduit flow in karst aquifers, *Journal of hydrology*, *378* (3): 230-239.

Luhmann, A. J., Covington, M. D., Peters, A. J., Alexander, S. C., Anger, C. T., Green, J. A., Runkel, A. C. and Alexander, E. C. (2011) Classification of Thermal Patterns at Karst Springs and Cave Streams, *Groundwater, 49*: 324–335.

Luhmann, A. J., Covington, M. D., Alexander, S. C., Chai, S. Y., Schwartz, B. F., Groten, J. T., and Alexander Jr, E. C. (2012) Comparing conservative and nonconservative tracers in karst and using them to estimate flow path geometry, *Journal of Hydrology*, *448*: 201-211.

Manga, M. (1998) Advective heat transport by low-temperature discharge in the Oregon Cascades, *Geology*, *26*(9): 799-802.

Manga, M. (2002) Using springs to study groundwater flow and active geologic processes, *Annual Review of Earth and Planetary Sciences, 29*: 201–228.

Okay, A. I. (1989) Geology of the Menderes Massif and the Lycian Nappes south of Denizli, western Taurides, *Mineral Resources Exploration Bulletin*, 109: 37-51.

O'Sullivan, D. and Unwin, D. J. (2010) *Frontmatter, in Geographic Information Analysis, Second Edition*, John Wiley & Sons Inc, Hoboken, NJ, USA.

Peel, M. C., Finlayson, B. L., and McMahon, T. A. (2007) Updated world map of the Köppen-Geiger climate classification, *Hydrology and Earth System Sciences Discussions*, *4* (2): 439-473.

Rimmelé, G., Oberhänsli, R., Goffe, B., Jolivet L., Candan O. and Çetinkaplan, M. (2003) First evidence of high-pressure metamorphism in the cover series of the southern Menderes Massif: Tectonic and metamorphic implications for the evolution of SW Turkey, *Lithos*, 71: 19-46.

Robertson, A.H.F. (2000) Mesozoic-Tertiary Tectonic-Sedimentary Evolution Of A South Tethyan Oceanic Basin And Its Margins In Southern Turkey. In: Bozkurt, E., Winchester, J.A. & Piper, J.D.A. (Eds) Tectonics And Magmatism In Turkey And The Surrounding Area, *Geological Society*, London, Special Publications, 173: 353-384.

Smart PL, Dawans JM, and Whitaker F. (1988) Carbonate dissolute in a modern mixing zone, *Nature,* 335: 811–3.

Sengör, A.M.C., and Yilmaz, Y. (1981) Tethyan evolution of Turkey: a plate tectonic approach, *Tectonophysics, 75*: 181– 241.

Thornthwaite, C. W. (1948) An approach toward a rational classification of climate, *Geographical review*, 55-94.

Ward, A. D., and Trimble, S. W. (2003) *Environmental hydrology*. CRC Press. 502p.

Açık Yüzey Buharlaşma Rasatlarının Değerlendirmesi, Retrieved October 30, 2015, from :

http://www.mgm.gov.tr/veridegerlendirme/acik-yuzey-buharlasma.aspx#sfU

Aylık Alansal Normal Yağış Dağılımı, Yıllık Toplam, Retrieved October 30, 2015, from :

http://www.mgm.gov.tr/veridegerlendirme/aylik-normal-yagis-dagilimi.aspx#sfU

Esri, GIS Mapping Software, Solutions, Services, Map Apps, and Data, Retrieved October 2, 2015, from :

http://www.esri.com/

Ex-tech, Retrieved November 2, 2015, from :

http://www.extech.com/instruments/resources/manuals/ec400_um.pdf

Documentation, matlab, Retrieved November 30, 2015, from :

http://www.mathworks.com/help/matlab/ref/surf.html

Documentation, matlab, Retrieved November 30, 2015, from :

http://www.mathworks.com/help/matlab/ref/pcolor.html

Geographic Information Analysis, Second EditionPublished Online: 17 MAR 2010, Appendix A: Notation, Matrices, and Matrix Mathematics, Retrieved November 30, 2015, from :

http://onlinelibrary.wiley.com/doi/10.1002/9780470549094.fmatter/pdf

Global Data Explorer (Powered by GeoBrain), Retrieved October 30, 2015, from :

http://gdex.cr.usgs.gov/gdex/

Google Earth, Retrieved October 2, 2015, from :

https://www.google.com/earth/

GW_Chart (Version 1.29.0.0), Retrieved November 20, 2015, from :

http://water.usgs.gov/nrp/gwsoftware/GW_Chart/GW_Chart.html

Horiba U-52 Manual, Retrieved November 2, 2015, from :

http://www.horiba.com/fileadmin/uploads/Process-Environmental/Documents/U-50_Manual_revised_0409.pdf


İklim Sınıflandırması, Muğla, Retrieved October 30, 2015, from:

http://www.mgm.gov.tr/iklim/iklim-siniflandirmalari.aspx?m=MUGLA


Matlab, Retrieved November 30, 2015, from :

http://www.mathworks.com/products/matlab/features.html


Resmi İstatistikler (İllerimize Ait İstatistiki Veriler), Retrieved October 30, 2015, from :

http://www.mgm.gov.tr/veridegerlendirme/il-ve-ilceler-istatistik.aspx?m=MUGLA


Unesco Official Web-site, *International Legend For Hydrogeological Maps*, Retrieved October 30, 2015, from :

http://unesdoc.unesco.org/images/0015/001584/158459eo.pdf


Yıllık Toplam Alansal Yağış Verileri, Muğla, Retrieved October 30, 2015, from :

http://www.mgm.gov.tr/veridegerlendirme/yillik-toplamyagisverileri.aspx?m=mugla#sfB

# APPENDICES

## Appendix A. Data Processing Steps

The MATLAB R2013a can plot matrix images automatically by clicking related graph button in graphs menu right after data import.

The matrix production steps were listed below:

1. Enter MatLAB R2013a.
2. Click on "Import Data" button on the upper left corner in "HOME" toolbar.
3. Select the data worksheet that has been prepared for to be plotted.
4. Select data cells in matrix format and import selection.
5. Select matrix data in "workspace window".
6. Click on "PLOTS" toolbar and select "pcolor" or "surf" command botton.

Also, to produce matrices in a different way, the commands *surf()* or *pcolor()* can be typed in command window after step 5.

All photographs were taken in between April and September 2015 by Eray AVCI, the author of this thesis.

The author declares and confirms here that the idea of matrix method application on springs is his personal idea and was not taken from somewhere else. It was inspired from spectrum analysis in sound engineering as stated before and in this thesis it was applied for hydrogeologic spring analysis.

# Appendix B. Statistics

**Table B1: The statistical information of 25 weeks data.**

| Location Number | Average T (˚C) | Average SpC (mS/cm) | Average pH | | Location Number | Average T (˚C) | Average SpC (mS/cm) | Average pH |
|---|---|---|---|---|---|---|---|---|
| 49 | 24.49 | 39.79 | 8.07 | | 24 | 15.67 | 4.55 | 7.31 |
| 48 | 16.53 | 6.22 | 7.48 | | 23 | 15.86 | 5.51 | 7.31 |
| 47 | 15.78 | 5.72 | 7.33 | | 22 | 15.97 | 6.64 | 7.30 |
| 46 | 16.16 | 4.97 | 7.39 | | 21 | 15.96 | 6.78 | 7.30 |
| 45 | 16.44 | 7.39 | 7.34 | | 20 | 16.10 | 6.50 | 7.29 |
| 44 | 16.45 | 6.95 | 7.38 | | 19 | 16.06 | 6.08 | 7.29 |
| 43 | 15.81 | 4.48 | 7.38 | | 18 | 16.05 | 5.56 | 7.29 |
| 42 | 15.57 | 8.49 | 7.37 | | 17 | 16.02 | 5.37 | 7.30 |
| 41 | 15.75 | 10.07 | 7.34 | | 16 | 16.01 | 5.50 | 7.30 |
| 40 | 15.94 | 11.62 | 7.32 | | 15 | 15.94 | 5.07 | 7.30 |
| 39 | 15.61 | 8.68 | 7.34 | | 14 | 15.79 | 4.54 | 7.31 |
| 38 | 15.33 | 5.68 | 7.37 | | 13 | 16.03 | 5.36 | 7.31 |
| 37 | 15.58 | 7.90 | 7.36 | | 12 | 16.02 | 5.49 | 7.31 |
| 36 | 16.82 | 14.57 | 7.32 | | 11 | 16.06 | 5.94 | 7.30 |
| 35 | 16.95 | 17.03 | 7.28 | | 10 | 15.95 | 5.73 | 7.29 |
| 34 | 14.98 | 3.16 | 7.38 | | 9 | 16.00 | 4.96 | 7.31 |
| 33 | 14.78 | 1.66 | 7.40 | | 8 | 16.01 | 4.48 | 7.34 |
| 32 | 15.80 | 6.51 | 7.36 | | 7 | 16.07 | 4.99 | 7.31 |
| 31 | 15.62 | 6.32 | 7.32 | | 6 | 15.99 | 5.37 | 7.29 |
| 30 | 15.38 | 5.16 | 7.33 | | 5 | 15.88 | 3.82 | 7.32 |
| 29 | 15.13 | 3.09 | 7.36 | | 4 | 15.85 | 3.71 | 7.36 |
| 28 | 15.09 | 2.67 | 7.36 | | 3 | 15.82 | 3.25 | 7.34 |
| 27 | 15.04 | 1.90 | 7.37 | | 2 | 15.80 | 2.46 | 7.34 |
| 26 | 15.05 | 1.96 | 7.41 | | 1 | 15.82 | 1.88 | 7.37 |
| 25 | 16.08 | 8.92 | 7.32 | | | | | |

**CURRICULUM VITAE**

**Personal Information**

Name Surname   : ERAY AVCI

Birth Of Date      : 1987

Nationality         : Turkey (TR)– Bulgaria (BG)

Email Address    : eryavci@gmail.com

Phone Number   : +905369897785

**Education**

2016 M.Sc. Geology Engineering, Muğla Sıtkı Koçman University, Muğla, Turkey.

2012 B.Sc.  Hydrogeology Engineering, Hacettepe University, Ankara, Turkey.

2010 B.Sc.  Earth Sciences, Johannes Gutenberg University, Mainz, Germany.

2005 High School, Gebze Anatolian High School, Gebze, Turkey.

**Skills**

Computer Programs-Languages:

Microsoft Office   : Good

ArcGIS                 : Good

MatLAB               : Good

C, C#                    : Good

**Scholarships**

2015 - TUBITAK – 2210-C Scholarship programme for M.Sc. Students

2010 - Erasmus Scholarship in Germany

2006-2010 - Vehbi Koç Foundation Scholarship for Academic Success

**Publications**

A Portable Water Temperature Logging Device For Field Use, Poster Presentation,
2015- JMO- 68th Turkish Geology Conference-Water For Nature And Society. MTA.

**Conferences And Courses Attended**

2015- JMO- 68th Turkish Geology Conference-Water For Nature And Society. MTA.

2014 - ISEM- 8.th International Symposium On Eastern Mediterranean Geology, Muğla Sıtkı Koçman University.

2010- World Water Crisis Course - (Water Policies In The Future) Johannes Gutenberg University – Mainz-Germany


**Languages And Certificates**

Turkish: Native Speaker

English: TOEFL IBT Score:  82 (2014 – San Diego, USA) , YDS Score: 80

German: A1, Certificate Johannes Gutenberg University (Germany, 2010)

Johannes Gutenberg University- 07.2010

Wiesbaden (Germany) – Water Treatment Plant Field

Kaplan International– San Diego USA – Advanced Certification


**Work Experience**

2014 - ISEM- 8.th International Symposium On Eastern Mediterranean Geology, Muğla Sıtkı Koçman University. Staff Member.

2011- Internship Field Engineer – DSI – The Water Institution Of Turkey.

Ankara (Etlik-Headquarters)- Turkey

2011- Internship Field Engineer: Çankırı, Kurşunlu, Kızlaryolu Dam Drilling site and Ankara, Yenimahalle, Alacatlı, Ümitköy, water well drilling site – DSI


**Personal Interests**

Electronics, Data logging systems, microprocessors and programming.